

UNCLASSIFIED

AD NUMBER

AD269748

LIMITATION CHANGES

TO:

Approved for public release; distribution is unlimited. Document partially illegible.

FROM:

Distribution authorized to U.S. Gov't. agencies and their contractors;

Administrative/Operational Use; 04 DEC 1961.

Other requests shall be referred to Office of Naval Research, One Liberty Center, 875 North Randolph Street, Arlington, VA 22203-1995.

Document partially illegible.

AUTHORITY

ONR ltr dtd 9 Nov 1977

THIS PAGE IS UNCLASSIFIED

UNCLASSIFIED

AD 269 748

*Reproduced
by the*

**ARMED SERVICES TECHNICAL INFORMATION AGENCY
ARLINGTON HALL STATION
ARLINGTON 12, VIRGINIA**



UNCLASSIFIED

DISCLAIMER NOTICE

THIS DOCUMENT IS THE BEST
QUALITY AVAILABLE.

COPY FURNISHED CONTAINED
A SIGNIFICANT NUMBER OF
PAGES WHICH DO NOT
REPRODUCE LEGIBLY.

NOTICE: When government or other drawings, specifications or other data are used for any purpose other than in connection with a definitely related government procurement operation, the U. S. Government thereby incurs no responsibility, nor any obligation whatsoever; and the fact that the Government may have formulated, furnished, or in any way supplied the said drawings, specifications, or other data is not to be regarded by implication or otherwise as in any manner licensing the holder or any other person or corporation, or conveying any rights or permission to manufacture, use or sell any patented invention that may in any way be related thereto.

STANFORD UNIVERSITY
STANFORD, CALIFORNIA

STANFORD ELECTRONICS LABORATORY

10

HD 269748

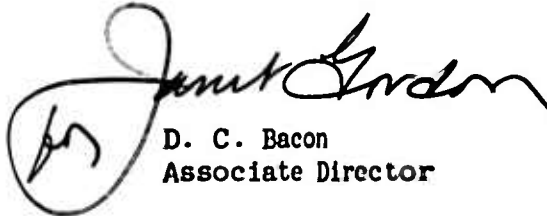
January 15, 1962

TO: ~~(The University)~~ Tepee Distribution

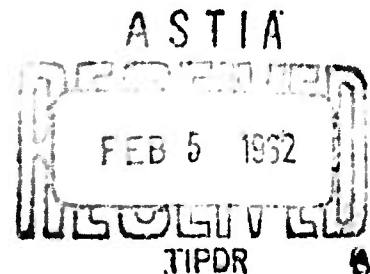
FROM: ~~(The University)~~ Publications Department

Re: ~~(The University)~~ Error noted in Stanford Electronics
~~(The University)~~ Laboratories Technical Report No. 45
~~(The University)~~ prepared under Contract Nonr 225(33)

Please ~~destroy~~ ~~over-~~ve and destroy pp. 9 - 10 from TR No. 45
and ~~replace~~ ~~with~~ the corrected pp. 9 - 10 enclosed
herewith.


D. C. Bacon
Associate Director

Enclure



III. EXPERIMENTAL OBSERVATIONS OF SOLAR FLARES AND SUBFLARES

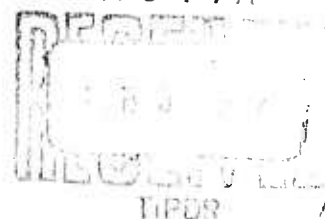
A. INTRODUCTION

Figure 2 shows a map of the United States and the area around Puerto Rico, showing location of the transmitting and receiving sites which will be referred to in this report. One of the transmitting stations, that of the National Bureau of Standards, is located near Washington, D.C. The 20-Mc transmission, called WWV-20, was monitored at the University of Washington (UW), Seattle, Washington, and at Stanford University (SU), Stanford, California. The other transmitting station is located at Mayaguez, Puerto Rico (PR) and has been operated by the University of Puerto Rico. The UW site has been monitoring the 18- and 10-Mc transmissions* and the SU site has been monitoring the 18-, 15-, and 10-Mc transmissions*. Station WWV-20 is off the air for 4 min, starting 45 min after each hr. The PR transmissions are interrupted every 2 min for 3 sec, and every 15 min for 30 sec. These time marks appear as negative spikes on the instantaneous-frequency paper records and can also be recognized in the amplitude, angle-of-arrival, and phase records. In addition, the transmitters are keyed with the identification letters every half hour.

Ray paths between the transmitting and receiving sites are also drawn in Fig. 2, together with their "reflection" points for 1-, 2-, and 3-hop propagation modes.

The instantaneous-frequency records have a full scale of 10 cps (2 cps/cm); the phase records have a full scale of 32π electrical radians. The angle-of-arrival records (with a few exceptions, which are so marked) have a 20-deg full-scale spatial spread. Amplitude is recorded with many sensitivities (0.2 v/cm to 2 v/cm). All recorders were run at a speed of 2.5 mm/min (about 6 in./hr), except the phase recorders which were run at 1 mm/sec.

*The exact transmitted frequencies from PR are 17.8825, 15.1025, 9.7675, and 9.7575 Mc.



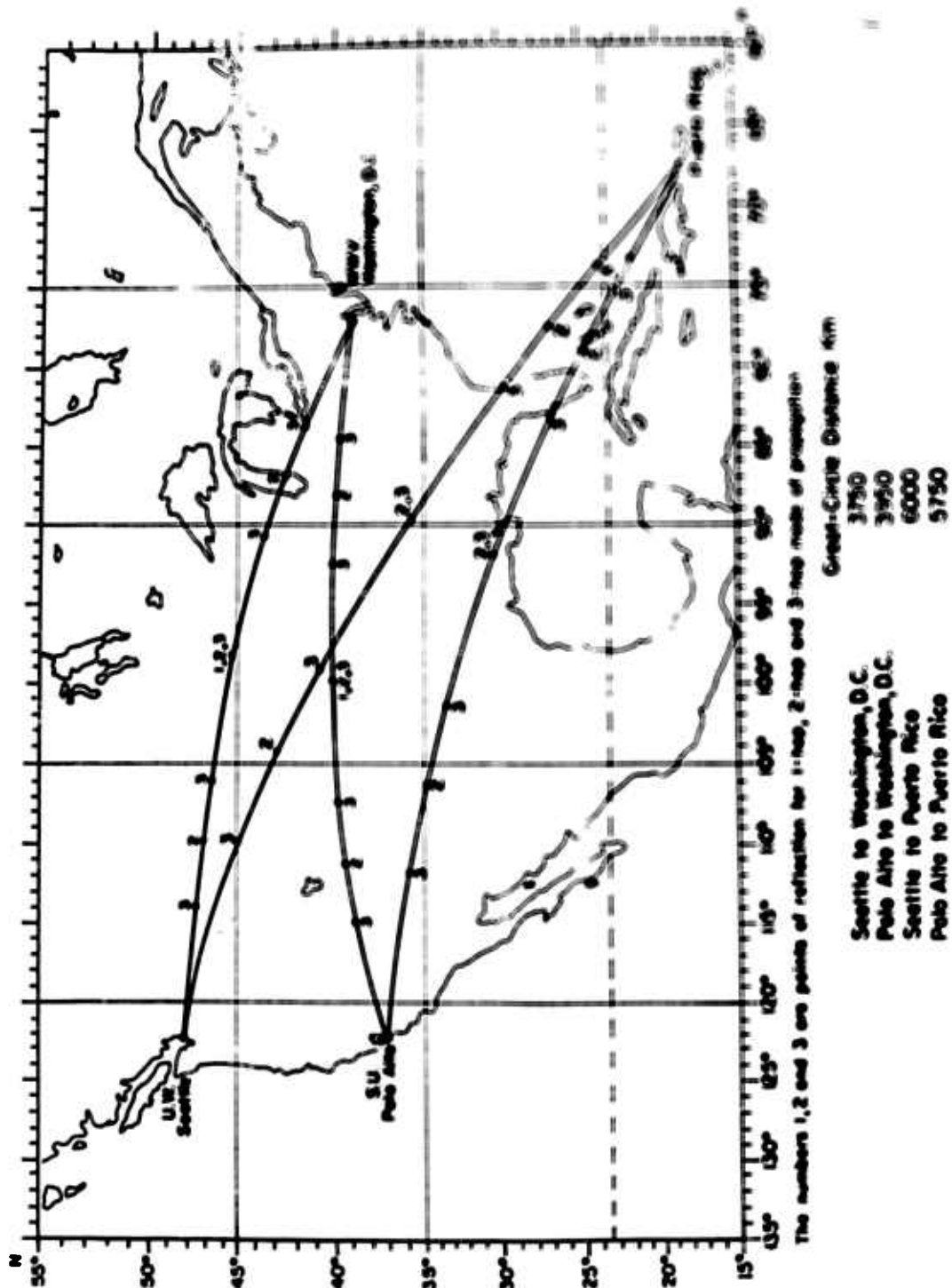


FIG. 2. GREAT-CIRCLE PATHS JOINING TRANSMITTING AND RECEIVING SITES.

XEROX

**The Altitude at which Solar-Flare-Induced
Ionization is Released**

by
D. P. Kanellakos and O. G. Villard, Jr.

4 December 1961

Technical Report No. 45



**PREPARED UNDER
OFFICE OF NAVAL RESEARCH CONTRACT
N0NR 225 (33)1, NR 04 003, AND
ADVANCED RESEARCH PROJECTS AGENCY, ARPA ORDER 196-61**

**RADIO SCIENCE LABORATORY
STANFORD ELECTRONICS LABORATORIES**

STANFORD UNIVERSITY • STANFORD, CALIFORNIA

NO. OTS



THE ALTITUDE AT WHICH
SOLAR-FLARE-INDUCED IONIZATION IS RELEASED

by

D. P. Kanellakos and O. G. Villard, Jr.

4 December 1961

Reproduction in whole or in part
is permitted for any purpose of
the United States Government.

Technical Report No. 45
Prepared under
Office of Naval Research Contract
Nonr 225(33), NR 088 003

Radioscience Laboratory
Stanford Electronics Laboratories
Stanford University Stanford, California

ERRATA

Page

12 Fig. 3 time scale should read: 1700 1733 1800 1830

27 Fig. 14, Note on Channel B should read: CHANNEL B: RELATIVE PHASES

29 Line 5 should read: frequency-analyzed, the incoming spectrum is split on the record.

41 Eq. (18) should read: $\Delta\omega = \pm u_n \beta - \int_A^B \frac{\partial\beta}{\partial t} ds$

(a) (b)

42 Right-hand side of equation should read: $1 \mp (\omega_H/\omega) |\cos \theta|$

49 Last entry of Table 2 should read: 2530 End

ABSTRACT

During the occurrence of certain solar flares and subflares (about 25 percent of those reported), the instantaneous frequency of a highly stable, c-w, h-f signal transmitted obliquely through the ionosphere is momentarily changed by a few cycles. The change consists of an increase in the frequency, followed by a decrease and subsequently a gradual return toward the original-received frequency. The rapid part of the frequency variation lasts only a few minutes (usually less than 5). In addition, the frequency change varies inversely with the operating frequency. Paths separated by many hundreds of kilometers are simultaneously affected. It is of interest that these pronounced frequency shifts invariably occur prior to the loss of signal characteristic of a short-wave fadeout, and hence could conceivably be used to warn of impending signal loss in modern h-f communication systems affording continuous feedback of propagation conditions over the path. In certain cases, however, the flare-induced frequency shift is not followed by a fadeout.

The azimuthal angle of arrival of the same signals that suffer frequency changes during solar flares and subflares also deviates in about one-third of the cases. The fact that an h-f wave suffers bearing deviations signifies that ionization is able to bend it. Electron-density gradients are probably produced from the solar-flare-induced ionization, especially at times when the sun's energy falls at a grazing angle on the path. The angle usually deviates to the south of the great-circle path in the case of the Puerto Rico - Palo Alto (PR - SU) path during the season at which these measurements were made.

These observations of instantaneous frequency and angle-of-arrival changes during solar flares suggest that new ionization is introduced initially somewhere just above the E region--very probably in the height region 120 to 140 km, although even higher heights are possible. This initial ionization may or may not be followed by the generation of ionization in the absorbing D region.

The time variation of height at which solar-flare-induced ionization is released, suggests that the ionization-producing radiant energy is initially soft, and then "hardens" as the flare progresses.

CONTENTS

	Page
I. Introduction and Historical Re . . .	1
II. Equipment for Experimental Mea . . .	6
III. Experimental Observations of S . . .	9
A. Introduction	9
B. Observed Effects	
1. Frequency Changes with	
2. Frequency Change Follo	
3. Phase and Amplitude Ra	
Solar-Induced Changes.	
4. Frequency Changes Foll	
5. Two-Hour Period During	
Subflare Produced Chan	
6. Two Solar Flares: The	
by More Severe Absorpt	
7. Two Solar Flares of Im	
Widespread Changes . .	
8. Solar Flare Inducing F	
no Absorption.	
9. Signal Enhancement Dur	
Maximum Phase.	
10. Short-lived Azimuthal	ar Fl
11. Simultaneous Absolute	e Rap
Run Records of Solar-II.	
12. Absolute Phase and Amplitude Rapid-Run Records	
Depicting Solar-Flare and Subflare-Induced Effe	
C. Spectrum Analysis of Short-Period Frequency	
Fluctuations	
1. Solar-Flare-Induced Fluctuation--No Mode	
Frequency Splitting.	
2. Fluctuation Caused by a Sudden Commencement--	
Mode Frequency Splitting	
3. Fluctuation During a Large Geomagnetic-Field	
Change--Mode Frequency Splitting and Continued	
Frequency Oscillations	
4. Fluctuation Caused by a Sudden Impulse-	
Frequency Splitting Occurring Simultane	
Widely Separated Paths	
IV. Theoretical Considerations and Experimental Ana	
A. Mathematical Model	
B. Frequency and Phase Variations	
C. Fermat's Principle	
D. Frequency Variations When ω_N Only Varies wi	

CONTENTS (Cont'd)

	Page
E. Frequency Variations when ω_1 Only Varies with Time. . .	43
F. Calculations of Attenuation when ω_1 Varies with Time. .	45
G. Analysis of the Induced-Effects of the 28 September 1961 Solar Flare of Importance 3	48
II. Agreement of Theoretical and Experimental Results . . .	51
V. Conclusions	53
Acknowledgments	54
References	55

Table	
1	Historical review of solar-flare-induced effects on the ionosphere
2	Occurrence of events of flare of 28 September 1961.

ILLUSTRATIONS

Figure	Page
1	Experimental setup for measuring absolute phase and amplitude of h-f signals.
2	Great-circle paths joining transmitting and receiving sites
3	Example of frequency changes accompanied with no absorption, for solar subflare of 14 August 1961.
4	Example of frequency change followed by slight absorption, for solar flare of 15 August 1961
5	Phase and amplitude rapid-run recordings showing details of solar-induced changes of Figs. 3 and 4
6	Example of frequency changes followed by severe absorption, for solar flare of 3 September 1961
7	Example of two-hour period on 4 September 1961 during which every reported solar flare and subflare produced changes
8	Examples of two solar flares of 4 September 1961, the less important one followed by more severe absorption.
9	Two solar flares of importance 1 inducing widespread, and different, frequency and bearing changes, 13 August 1961. . .
10	Example of solar-flare induced frequency changes but no absorption.
11	Example of signal enhancement during solar-flare maximum phase, 15 June 1961.
12	Example of short-lived azimuthal-bearing change during solar flare, 29 July 1961, showing effects on widely separated signal paths.

ILLUSTRATIONS (Cont'd)

Figure	Page
13 Simultaneous phase and amplitude rapid-run records showing detailed changes induced during solar flare of importance 3, 28 September 1961	25
14 Effects of solar flares on phase and amplitude of 18-Mc FR-SU signal, 30 August 1961.	27
15 Effects of solar subflares on phase and amplitude of 18-Mc FR-SU signal, 25 August 1961.	28
16 Frequency analysis of total received frequency spectrum of solar-flare-induced frequency fluctuation, 4 December 1960. Frequencies of all incoming modes affected by same amount . .	30
17 Frequency analysis of total received frequency spectrum of frequency fluctuation caused by SC, 24 October 1961. Frequencies of the many incoming modes affected by different amounts.	31
18 Frequency analysis of total received frequency spectrum of frequency fluctuation during large geomagnetic-field fluctuation, 28 March 1961. Frequencies of the many incoming modes affected by different amounts	33
19 Frequency analysis of total received frequency spectrum of frequency fluctuation caused by SI, 4 February 1961. Frequencies of the many incoming modes affected by different amounts simultaneously over widely separated paths.	34
20 Simplified wave-path geometry	39
21 Collision frequency vs height.	47

LIST OF SYMBOLS

$\omega = 2\pi f$	operational angular frequency, radians/sec
$\lambda = \frac{c}{f}$	wavelength, in free space, of h-f wave of frequency ω
$\gamma = \alpha + j\beta$	propagation function/m
α	attenuation function (nepers/m)
β	phase function (radians/m)
$\beta_v = \frac{\omega}{c}$	propagation function of vacuum (radians/m)
$\omega_{pi} = 2\pi \sqrt{\frac{N e^2}{m}}$	angular plasma-resonance frequency (radians/sec)
$\omega_{ci} = \frac{\mu_v e H}{m}$	angular gyrofrequency (radians/sec)
μ_v	permeability of vacuum (henrys/m)
$\mu_v H = B$	geomagnetic field
B	geomagnetic field (webers/m ²)
e	charge of electron (coulombs)
m	mass of electron, kg
N	electron charge density (electrons/m ³)
ν	collision frequency (events/sec)
c	velocity of light in vacuum (m/sec)
θ	angle between the direction of propagation and the direction of the geomagnetic field (in our case 50 deg $\leq \theta$ 60 deg)
ψ	take-off angle of wave (deg)
ϕ	total phase of wave (a function of time) (radians)
u_n	component of the velocity along direction of propagation
v_p	phase velocity of wave of frequency ω
v_g	group velocity of the wave of frequency ω
n	refracting index of ionosphere
A	power absorption of signal (db)

l	phase (cycles)
S	path length
τ	time delay
h'	virtual height

I. INTRODUCTION AND HISTORICAL REVIEW

Since the early days of h-f radio propagation, students of the ionosphere have been confronted with the influence of the sun upon it. The sudden occurrence of fading or disappearance - the so-called Short-Wave Fadeout (SWF) - of h-f signals obliquely transmitted through the ionosphere was first noticed by Mögel [Ref. 1] in 1930. Later, Dellinger [Ref. 2] was the first to associate these Sudden Ionospheric Disturbances (SID's) with the simultaneous eruptions (solar flares) taking place in the sun. Thus, the so-called Mögel-Dellinger effect became an object of intense study by the many workers in the h-f ionospheric propagation field. Table 1 presents a condensed history of the observations of the effects of solar flares on the upper atmosphere by the main workers in the field.

The various workers used different methods and equipment for measuring the changes in the ionospheric parameters that could be affected by the changes brought about by solar flares. The interpretations and conclusions reached from experimental observations of the ionosphere were often limited by the scope of the experiments. Many workers held completely opposite views and reached contradictory conclusions as to what really happened in the ionosphere during solar flares. Martyn, Munro, Higgs and Williams [Ref. 3], for example, by studying certain anomalies appearing on vertical-incidence ionograms during solar flares, noticed that the virtual height of the ionospheric, F-region reflection point rose following a solar flare. They attributed this to an actual upward movement of the F layers and a decrease of the electron density of these layers, often somewhat before absorption effects appeared near the reflecting point.

The above observations were contrary to the earlier statements by Dellinger [Ref. 4], McNish [Ref. 5], and others [Refs. 6,7,8,9,10], who had postulated that most of the effects are concentrated in the D region (below 90 km). In 1938, Burkard [Ref. 11], by studying the ionosphere with signals of 30 Mc, concluded that the ionization increase was entirely in the E region. An interesting experimental result was reported by Naismith and Beynon [Ref. 12]. By studying the vertical reflections

TABLE 1 HISTORICAL REVIEW OF SOLAR FLARE-INDUCED EFFECTS
ON THE IONOSPHERE

Year	Reported by*	Observation or Discovery
1921 to 1930	H. Meiss (1)	First reported fadeouts on communication h-f circuits.
1932 to 1935	J. H. Dellinger (2)	First associated fadeouts with "Solar Eruptions."
1929 to 1931	R. Bureau (3)	First reported SEA effects on vlf during solar flares.
1931	J. H. Dellinger (4)	Attributed effects of solar flares in D region; coined term "SID."
1931	A. G. McNish (5)	Agreed with Dellinger that solar flares affect 60 to 100 km portion of ionosphere. Studied magnetic phenomena.
1931	D. F. Martyn, et al. (6)	Reported decrease in F-region ionization during solar flares. F-layer moves down.
1938	O. Hufnagel (11)	Reported ionization increase during SID entirely in E region (used $f = 30$ Mc).
1938	R. N. Smith and and W. J. G. Heyman (12)	Stated solar flare of importance 1 produced short-lived ionization at 125 km.
1938	B. Beckman, W. Menzel and F. Visking (13)	Reported that E and F regions are affected. D-region picture inadequate.
1939	H. N. Bracewell and I. W. Starker (14)	Reported reflecting layer of vlf moves down (D region). SPA log solar flares.
1950	W. Becker and W. Dieringer (15)	Reported F-region ionization increases during a strong flare. F-layer moves down.
1951	K. Bibl (17)	Stated changes in $f_oE > 0.2$ Mc correlate quite well with SID.
1951	J. W. Findlay (18)	Stated that maximum ionization during fadeouts 100 \pm 2 km.
1953	M. A. Ellison (19)	Reported SEA's log solar flares by 1 to 10 min with average of 5 min.
1954	A. P. Mitra and R. E. Jones (29)	Stated there is no evidence of an increase in recombination coefficient during an SID.
1958	C. M. Minnis and G. H. Barzard (16)	Reported F-region ionization increases during strong solar flares. F-layer moves down.
1960	H. C. Fenwick and O. G. Villard, Jr. (20)	Observed short period increases in instantaneous frequency.
1960	K. i. Chan, O. G. Villard, Jr., and H. Duont (21)	Correlated these short-period frequency changes with solar flares.
1961	B. W. Knecht and K. Davies (22)	Reported frequency increases during a strong solar flare. F-region N_f goes up. F-layer moves down.
1961	P. H. Wideson and G. H. Barry (32)	Stated that frequency changes in backscatter during a flare do not force a downward moving layer.

*Number in parentheses corresponds to appropriate reference as given on pages 55, 56, 57.

of h-f signals from the F region without getting reflections from the E region, they noticed echoes suddenly appearing from a height of 125 km. These echoes lasted a few minutes at the end of which the F-layer echoes were seen again in their normal place. A solar flare of importance 1 took place during this short interval. The behavior of the ionosphere during this flare was the same as that which will be reported later in this paper. Beckman, Menzel, and Vilbig [Ref. 13] in the same year (1938) published a paper maintaining the D-region effects are inadequate to explain what happens in the ionosphere during solar flares. They thought the E and F regions were affected as well. Bracewell and Starker [Ref. 14] studied extensively the Sudden Phase Anomalies (SPA) produced on vlf transmissions (16 kc) during solar flares. They concluded that the D-region ionization is increased during solar flares. However, in 8 out of 12 cases reported in this paper the SPA's came after the times of the visible maxima of the flares. Beckner and Dieminger [Ref. 15] in 1950, and Minnis and Bazzard in 1958 [Ref. 16], reported that during a very strong solar flare that was accompanied by cosmic rays, the F-region ionization increased appreciably and the F layer moved downward. Bibl [Ref. 17] reported in 1951 that increases in the E-region critical frequency of more than 0.2 Mc were taking place during SID's. In the same year Findlay [Ref. 18], by studying the changes of the phase and group paths of 2-Mc signals during SID's, concluded that the maximum ionization during fadeouts is produced at a height of 101 ± 2 Km. Ellison [Ref. 19] published a paper in 1953 in which he reported that the Sudden Enhancements of Atmospherics (SEA's) invariably lag the time of the maxima of solar flares by 2 to 10 min.

It is evident from this brief review that no agreement has been reached as to where the maximum ionization is usually first produced.

Coming now to the group of references that more closely relates to our work, we notice that short-period increases followed by decreases in the instantaneous-received frequency of highly stable h-f waves were first observed by Fenwick and Villard [Ref. 20] in 1960. They speculated that these rather sudden changes in the instantaneous-received frequency might be due to rapidly downward-moving F-region irregularities. Later in the same year Chan, Villard, and Dueño [Ref. 21] associated

these short-period changes in the instantaneous frequency with solar flares occurring simultaneously with the changes. Similar effects have been published more recently by Knecht and Davies [Ref. 22]; they found an F-region increase in ion density and speculated that the change in the instantaneous frequency could be due to a downward movement of the F-region layer during a strong solar flare. However, close examination of the effect of solar flares on the instantaneous-received frequency of h-f waves obliquely propagated through the ionosphere over long paths, has brought to light certain evidence which strongly suggests that the ionosphere is affected above the E region first, and that the D region may or may not be affected later.

During the occurrence of certain solar flares and subflares the instantaneous frequency of highly stable c-w h-f signals transmitted obliquely through the ionosphere is momentarily changed by a few cycles. The change usually consists of an increase in the frequency, followed by a decrease and subsequently a gradual return toward the original-received frequency.

The rapid part of the frequency variation lasts only a few minutes (usually less than 5). In addition, the frequency changes vary inversely with the operating frequency. Thus, a downward-moving layer must be excluded since it would have produced changes that vary directly with the operating frequency (doppler effect). Paths separated by many hundreds of kilometers are simultaneously affected. These pronounced frequency shifts invariably occur prior to the loss of signal characteristic of a short-wave fadeout. (On some occasions, an increase in the signal is observed.) In certain cases, however, the flare-induced frequency shift is not followed by a fadeout. Moreover, the frequency changes lead the times of the maximum phase of the solar flare by 1 to 4 min. Finally, the azimuthal angle of arrival of the same signals that suffer frequency changes during solar flares and subflares is also changed in a few instances.

It is the intention of this report to show that solar flares often produce ionization in the ionosphere above the E level first, and then may or may not produce ionization in the absorbing D region at a later time. Most articles about SID's postulate changes no higher than the

D and E regions. Only during the very intense solar flares(those accompanied by cosmic rays) is there thought to be any change in the F region.

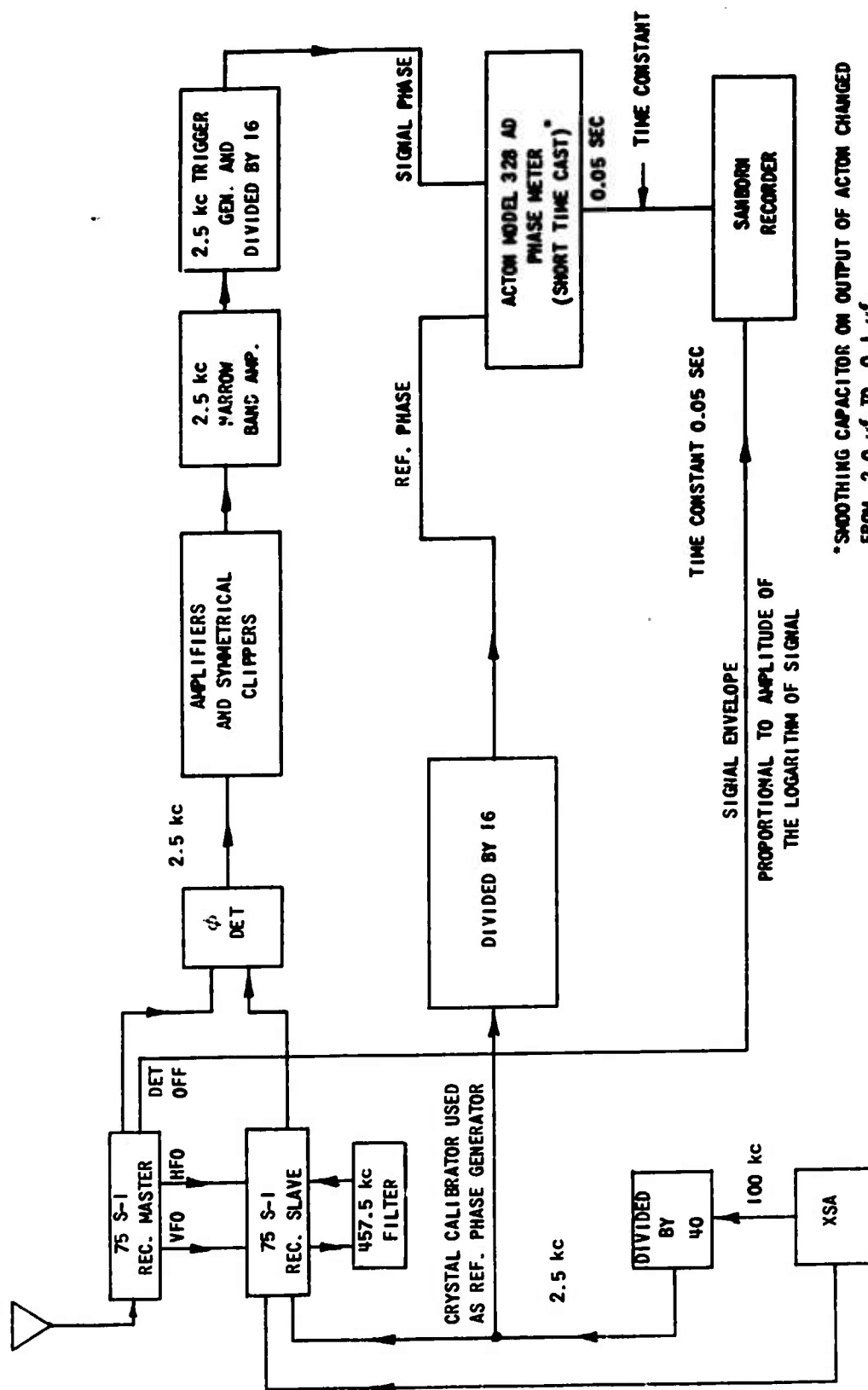
Chapter II discusses briefly the experimental setups used in measuring the results, Chapter III gives many examples of experimental results of solar-flare-induced ionization effects on h-f signal characteristics, and Chapter IV considers a simple theoretical model to explain and justify the experimental evidence.

II. EQUIPMENT FOR EXPERIMENTAL MEASUREMENTS

Detailed experimental setups for measuring instantaneous frequency and angle of arrival have previously been reported [Refs. 20,21,23,24]. This method of measuring the instantaneous frequency has been pioneered by the National Bureau of Standards [Ref. 23]. In brief, the frequency deviations were derived by comparing the locally generated standard frequency with the frequency of the transmitted signals. Standard-frequency sources at both receiving and transmitting sites were Rohde and Schwarz XSA standards, rated at 1 part in 10^9 maximum daily frequency drift and 1 part in 10 maximum hourly frequency drift.

The receiving standards were offset from the transmitting standard by about 5 cps. The resulting beat subaudio frequency was fed through a low-pass filter designed to eliminate hum and interference and into the recording apparatus. Recording was accomplished by feeding the amplified beat frequency into a frequency meter (HP-500B) whose output was recorded by (1) a Sanborn paper-tape recorder running at a speed of 2.5 mm/min on a routine basis, 24 hours a days, with a time constant of 5 sec; and (2) a direct-recording, Webcor magnetic-tape recorder modified to run at approximately 1/50 in./sec. The Sanborn recorder displays the beat frequency resulting from the strongest received signal component, while the Webcor records the entire received subaudio fading spectrum. When played at 15 in./sec, the tape recording gives a signal whose frequency falls within the input-acceptance frequency band of a Kay "Sona-Graph" or a Raytheon "Rayspan" a-f analyzer.

The angle of arrival of the same highly stable, c-w h-f signals is determined by a phase-comparison method. The phases of two identical Yagi antennas, transversely spaced to the true PR bearing 3λ apart, are compared with an Applied Technology Phase Tracking Interferometer (PTI-1) or a phase-comparison direction-finder consisting of a siamesed SP600 receiver pair. The phase-information output of the PTI-1 is recorded on a Sanborn recorder running at 2.5 mm/min, whereas that of the phase meter is recorded on an Esterline Angus ink-chart recorder running at 6 in./hr. The effective time constants of the recorders were 4 and 10 sec, respectively.



*SMOOTHING CAPACITOR ON OUTPUT OF ACTION CHANGED FROM 2.0 μf TO 0.1 μf .

FIG. 1. EXPERIMENTAL SETUP FOR MEASURING ABSOLUTE PHASE AND AMPLITUDE OF h-f SIGNALS.

The measurements of the phase and amplitude were made with an experimental setup shown in Fig. 1. The phase of incoming transmitted stable signal has been compared with that derived from a locally generated signal of the same stability (1 part in 10^9 per day). The comparison is accomplished in an Acton Model 328 AD phase meter. The output of the phase meter is integrated and fed into a Sanborn paper recorder which runs at 1 mm/sec. The full-scale reading is 32π electrical radians or 16 cycles (wavelengths). The incoming signal is, in addition, envelope-detected and fed into another channel of the same Sanborn recorder. The detected output is proportional to the logarithm of the amplitude of the incoming signal. The effective integration time constants for both phase and amplitude are 0.05 sec. (The AGC time constants of the 75 S-1 receivers were set at 3 sec.)

III. EXPERIMENTAL OBSERVATIONS OF SOLAR FLARES AND SUBFLARES

A. INTRODUCTION

Figure 2 shows a map of the United States and the area around Puerto Rico, showing location of the transmitting and receiving sites which will be referred to in this report. One of the transmitting stations, that of the National Bureau of Standards, is located near Washington, D.C. The 20-Mc transmission, called WWV-20, was monitored at the University of Washington (UW), Seattle, Washington, and at Stanford University (SU), Stanford, California. The other transmitting station is located at Mayaguez, Puerto Rico (PR) and has been operated by the University of Puerto Rico. The UW site has been monitoring the 18- and 10-Mc transmissions* and the SU site has been monitoring the 18-, 15-, and 10-Mc transmissions*. Station WWV-20 is off the air for 4 min, starting 45 min after each hr. The PR transmissions are interrupted every 2 min for 3 sec, and every 15 min for 30 sec. These time marks appear as negative spikes on the instantaneous-frequency paper records and can also be recognized in the amplitude, angle-of-arrival, and phase records. In addition, the transmitters are keyed with the identification letters every half hour.

Ray paths between the transmitting and receiving sites are also drawn in Fig. 2, together with their "reflection" points for 1-, 2-, and 3-hop propagation modes.

The instantaneous-frequency records have a full scale of 10 cps (2 cps/cm); the phase records have a full scale of 32π electrical radians. The angle-of-arrival records (with a few exceptions, which are so marked) have a 20-deg full-scale spatial spread. Amplitude is recorded with many sensitivities (0.2 v/cm to 2 v/cm). All recorders were run at a speed of 2.5 mm/min (about 6 in./hr), except the phase recorders which were run at 1 mm/sec.

*The exact transmitted frequencies from PR are 17.8825, 15.1025, 9.7675, and 9.7575 Mc.

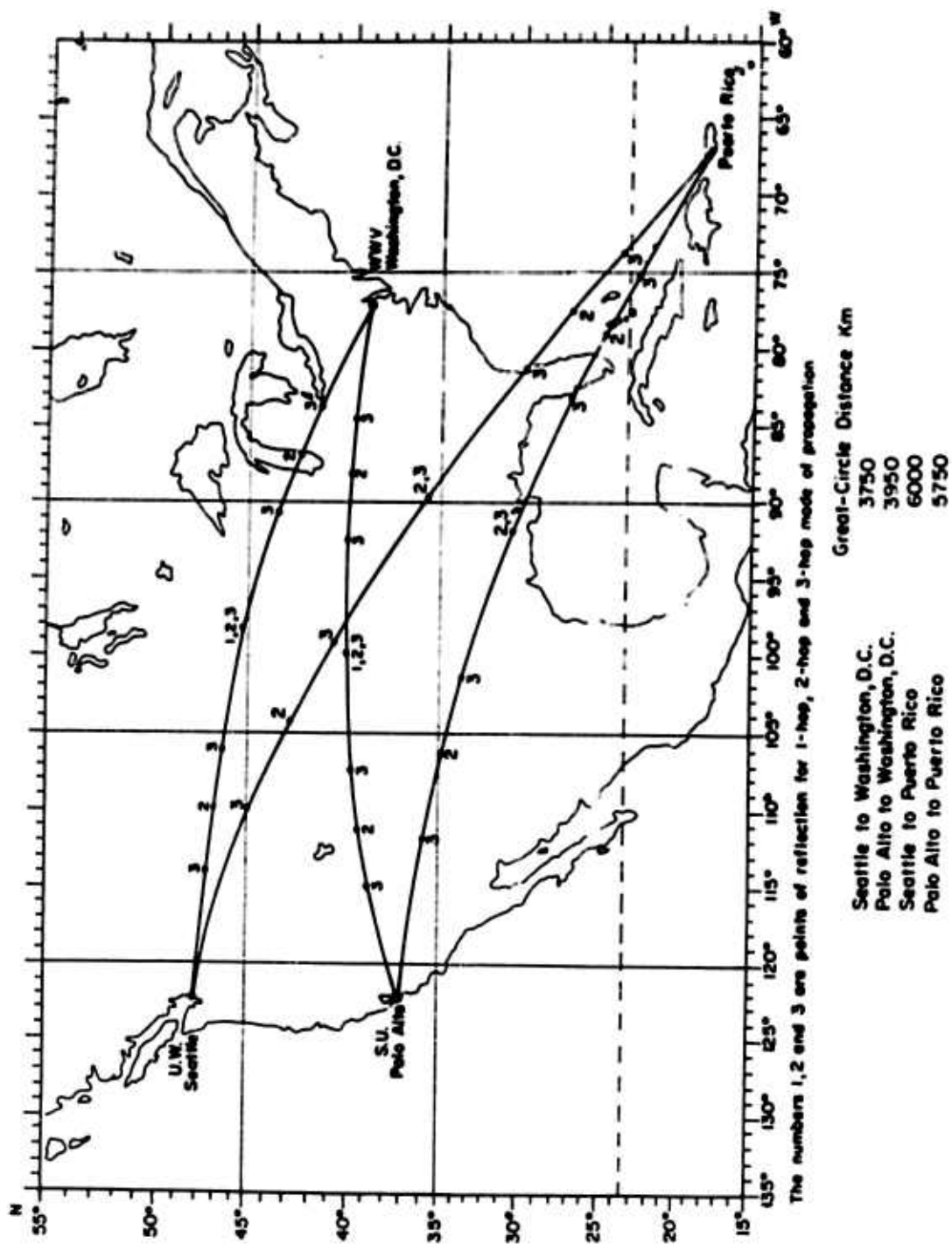


FIG. 2. GREAT-CIRCLE PATHS JOINING TRANSMITTING AND RECEIVING SITES.

B. OBSERVED EFFECTS

The following figures show many examples of the solar-flare-induced effects in the instantaneous frequency, absolute phase, angle of arrival, and amplitude of h-f waves.

1. Frequency Changes with No Absorption. Figure 3 shows the effect of the solar subflare 20 of 14 August 1961 on the WWV-20, FR-18, and FR-15 transmissions as monitored at the SU site. Notice the increases in the received frequency for each case at about 1731 to 1732*. This time corresponds to the reported [Ref. 25] solar subflare maximum phase during which the frequency change varies inversely with the operating frequency. Notice also that during this time interval (and also subsequently) the amplitude of the 15-Mc signal (that of the lowest of the three frequencies recorded) showed no observable absorption. (The sensitivity of the amplitude recording of the PTI-1 is about 3 to 4 db/cm.) The relative direction of the 15-Mc wave during the time of the frequency change was momentarily shifted south of the great-circle plane joining transmitter and receiver. Subsequently, the 15-Mc wave was deviating toward the north while its frequency was increasing.

2. Frequency Change Followed by Slight Absorption. Figure 4 shows the effect of the solar flare of importance 1 of 15 August 1961 on the same signals over the same paths of Fig. 3. Notice that the frequency changes at about 1947. The maximum of the frequency change occurs 2 min prior to the time [Ref. 26] of visual phase maximum of the solar flare. There is no change in the angle of arrival of the 15-Mc signal. Partial absorption commences at about 2 min after the maximum of the frequency change, and is about 6 db below the signal level at the time of the maximum frequency change. The signal attains this value 8 min after the maximum frequency change.

3. Phase and Amplitude Rapid-Run Recordings of Solar-Induced Changes Figures 5a and 5b show the details of the subflare and flare effects on the 18-Mc-signal amplitude and phase discussed in Figs. 3 and 4. In these figures, the slope of the phase is proportional to frequency

*Times throughout this report are given in Greenwich Mean Time (GMT).

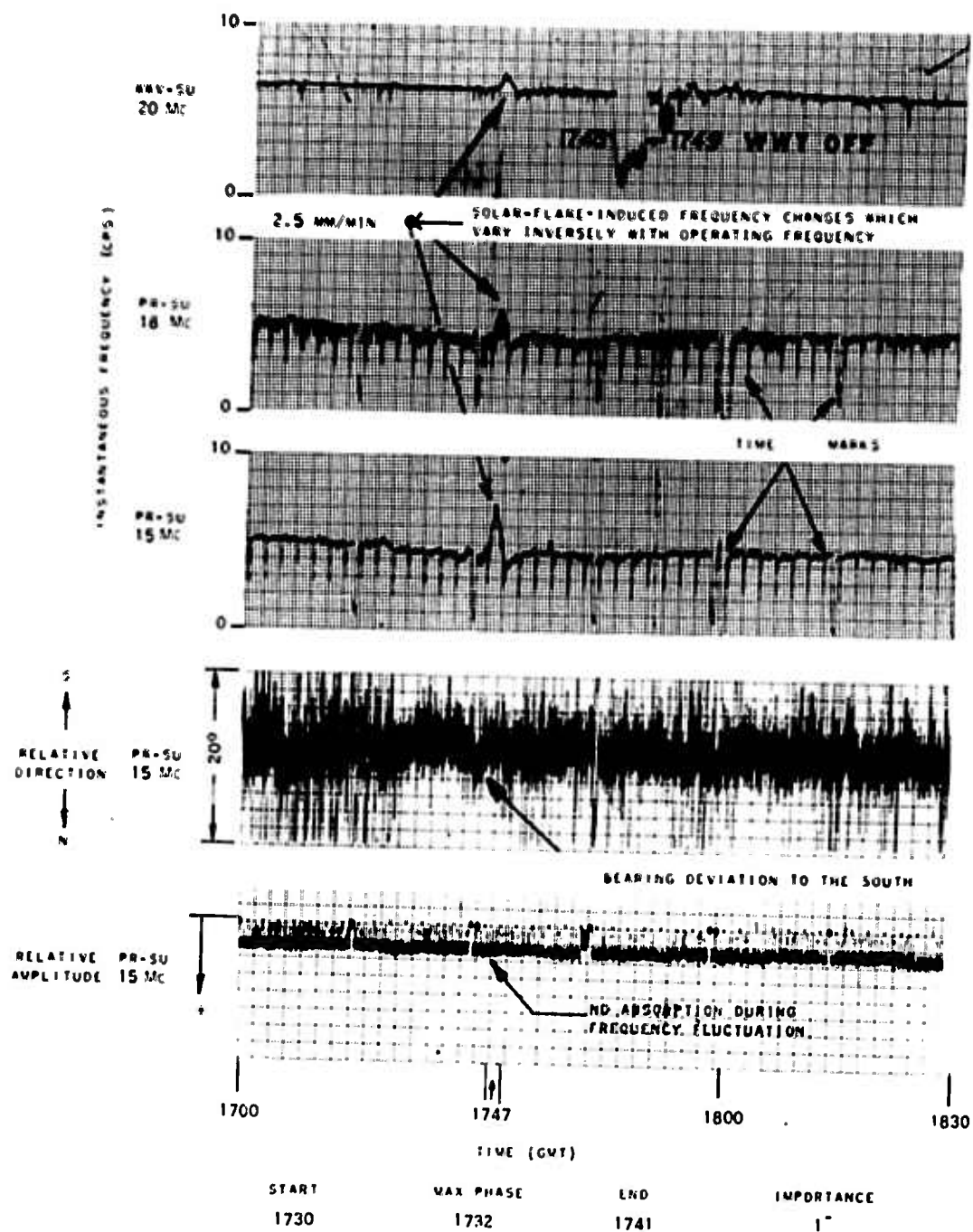


FIG. 3. EXAMPLE OF FREQUENCY CHANGES ACCOMPANIED WITH NO ABSORPTION, FOR SOLAR SUBFLARE OF 14 AUGUST 1961.

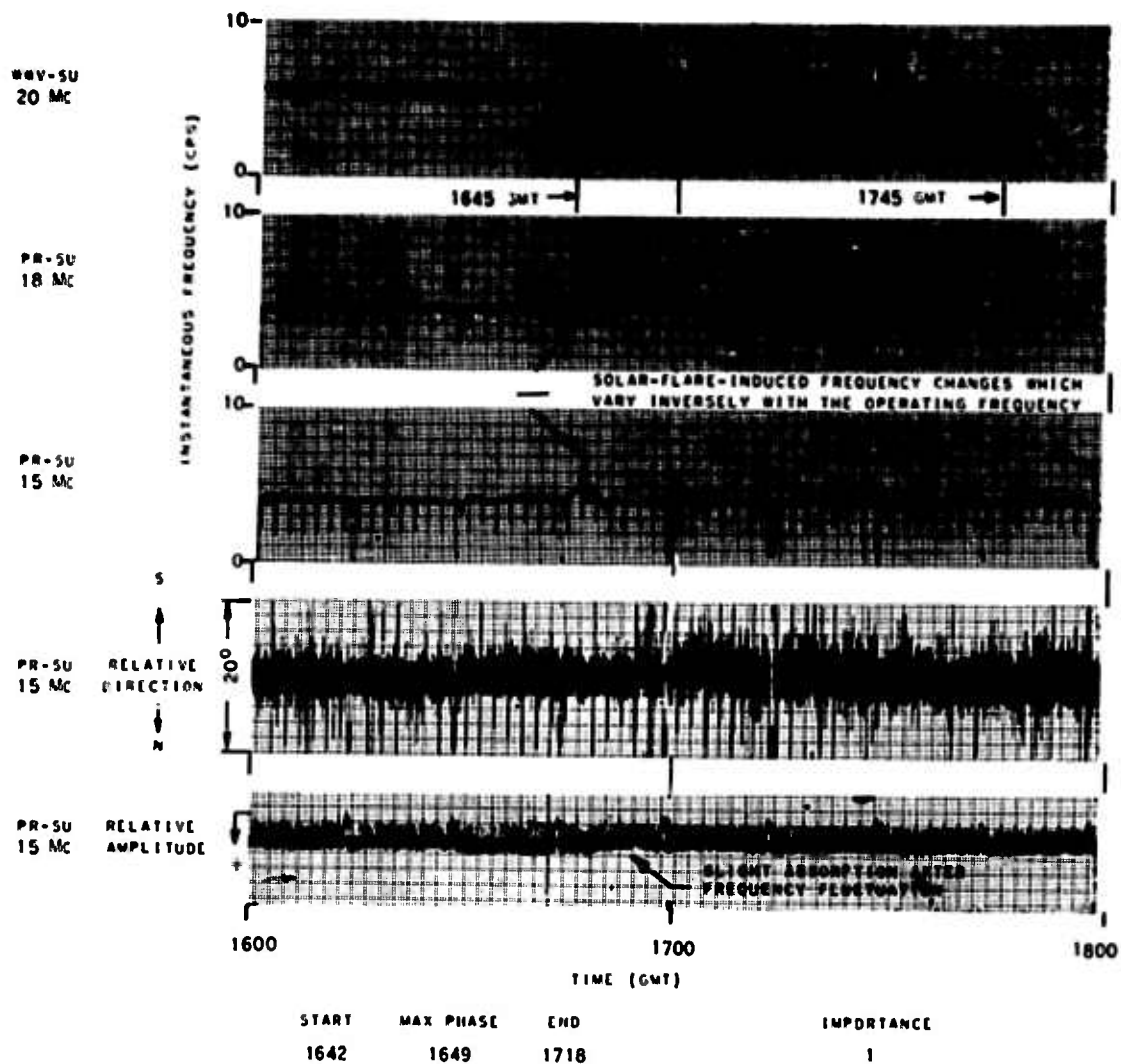


FIG. 4. EXAMPLE OF FREQUENCY CHANGE FOLLOWED BY SLIGHT ABSORPTION, FOR SOLAR FLARE OF 15 AUGUST 1961.

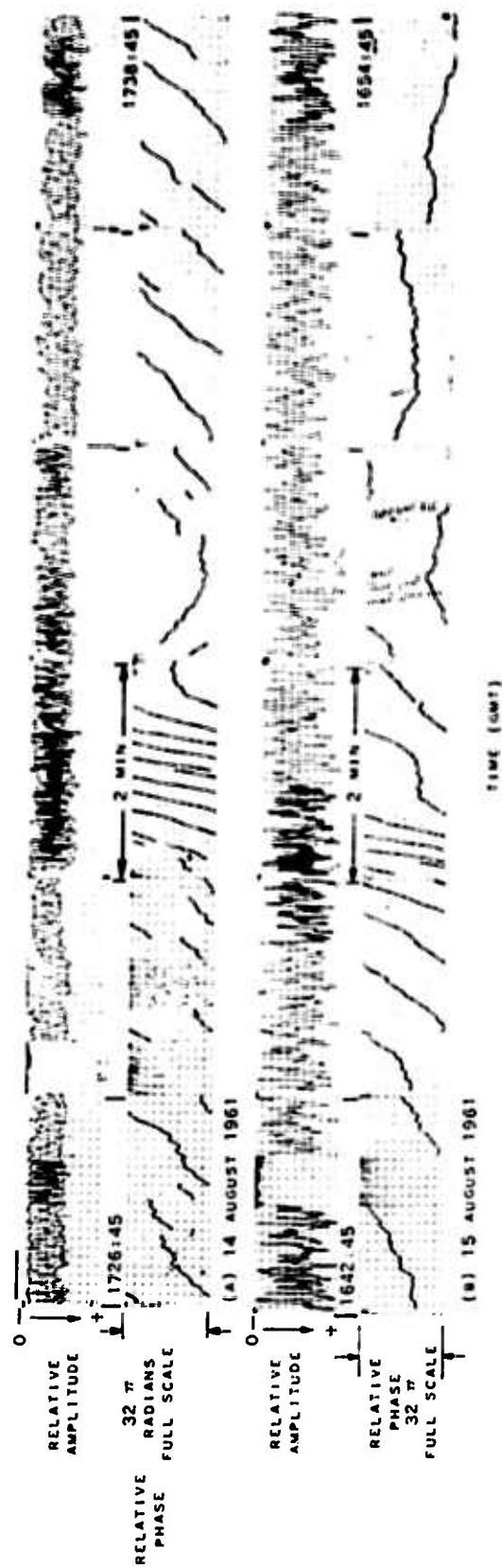


FIG. 5. PHASE AND AMPLITUDE RAPID-RUN RECORDINGS SHOWING DETAILS OF SOLAR-INDUCED CHANGES OF FIGS. 3 AND 4.

(i.e., $\omega = d\phi/dt$). In both cases, the slope increases, reaches a maximum, and then decreases. Subsequently, the slope passes through zero and finally becomes negative only to return to the normal (presolar) slope many minutes later. This elapse of time in returning to normal is characteristic of an F-region recovery time constant. The fading rate of the signal during the maximum phase change increased to twice the preflare value in both cases, whereas the signal amplitude barely changed. In addition, the subflare (Fig. 5a) produced more phase change than the flare of importance 1 (Fig. 5b).

4. Frequency Changes Followed by Severe Absorption. Figure 6 depicts the effect of the solar flare of importance 1 of 3 September 1961 on the frequency of the WWV-20 and PR-18 signals, and on the angle of arrival and amplitude of the PR-15 transmissions. The maximum frequency change in this case occurred at 2046, 5 min before the maximum phase of the flare. This was followed, however, by a second maximum at 2048. It is characteristic that in this case, unlike that of August 15, rather severe absorption of the h-f signal was observed. As in the previous case, however, the maximum absorption was reached after the maximum frequency change had taken place. There is a slight angle-of-arrival change during the time of the maximum frequency change for this case. The angle shifts momentarily toward the south of the path. The 15-Mc wave subsequently deviates southward right after the solar flare (actually during the negative phase) by 2 deg.

5. Two-Hour Period During Which Every Solar Flare and Subflare Produced Changes. Figure 7 shows the frequency changes, angle-of-arrival variation, and absorption produced by a series of solar subflares and flares occurring in a 2-hr period on 4 September 1961. The less pronounced effects are emphasized with arrows. Only the solar flare of importance 2 produced substantial, measurable absorption which, characteristically, commenced 1 min after the time of the maximum frequency excursion. All frequency variations are larger on the PR-SU 18-Mc than on the WWV-SU 20-Mc signal. During the time interval of the maximum frequency change at about 1915, the 15-Mc angle-of-arrival signal deviated about 1.5 deg to the south for a period of 2 min, or so.

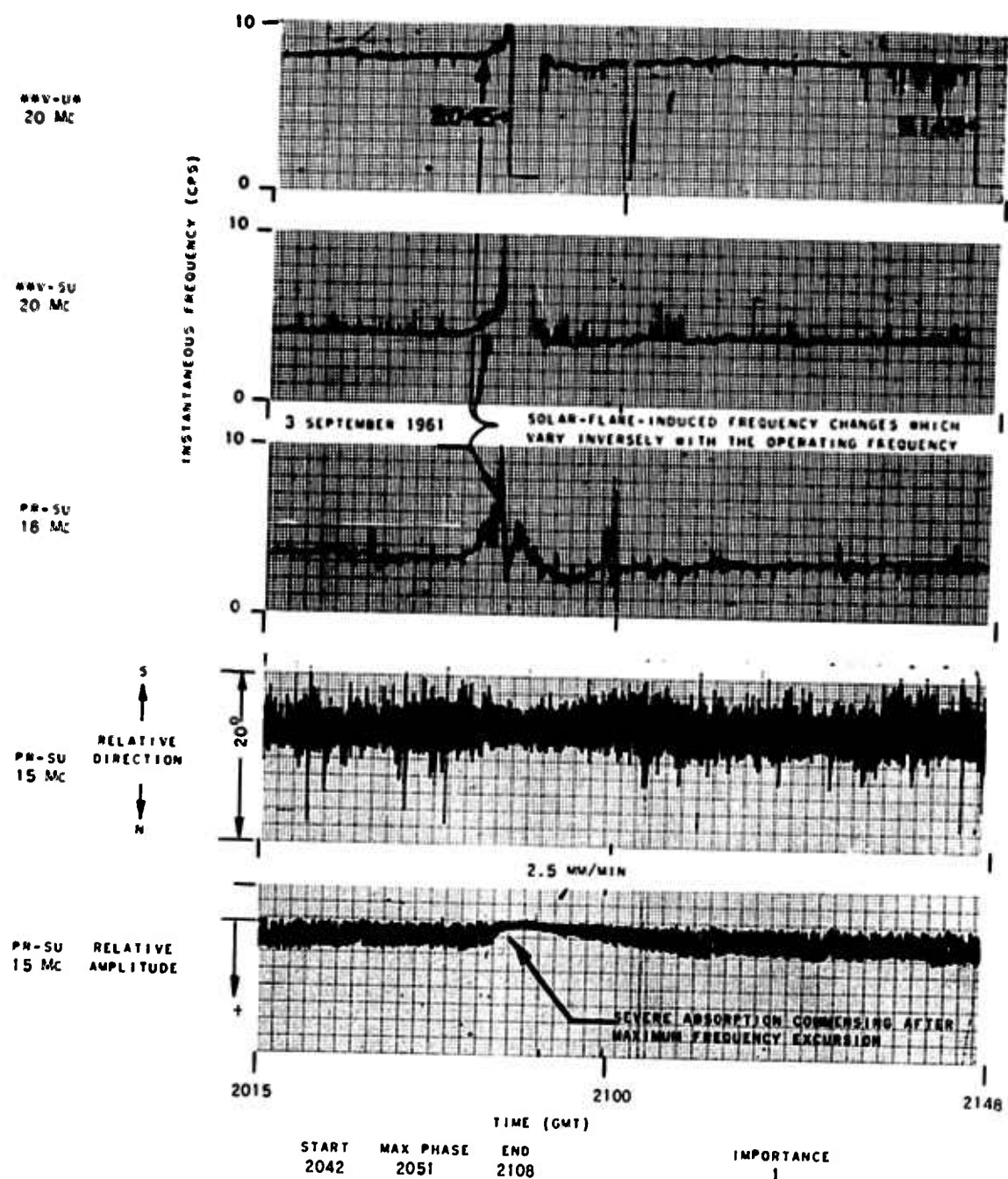
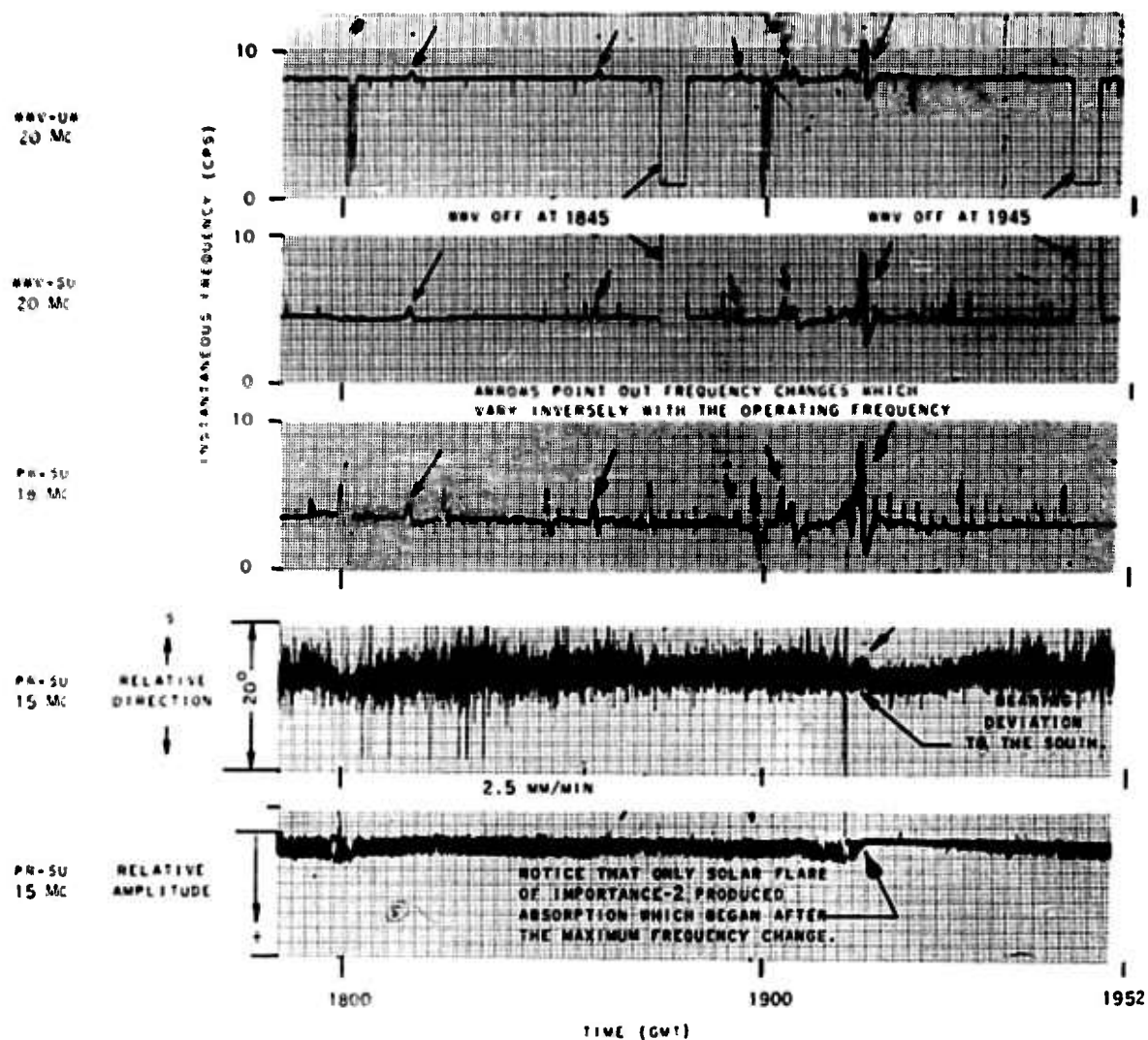


FIG. 6. EXAMPLE OF FREQUENCY CHANGES FOLLOWED BY SEVERE ABSORPTION, FOR SOLAR FLARE OF 3 SEPTEMBER 1961.



START	MAX PHASE	END	IMPORTANCE
1807	1810	1814	1-
1835	1843	1856	1-
1856	1857	1900	1-
1902	1905	1909	1
1911	1924	2018	2

FIG. 7. EXAMPLE OF TWO-HOUR PERIOD, ON 4 SEPTEMBER 1961, DURING WHICH EVERY REPORTED FLARE AND SURFLARE PRODUCED CHANGES.

Other flares and subflares of less importance produced an increase in the rate and amplitude of the angle-of-arrival scintillations. Figure 7 shows that on particular days when specific sunspot regions are active every flare and subflare produces frequency variations on the h-f signals. In general, however, only a small percentage (15 to 20 percent) of solar flares and a larger percentage (25 to 30 percent) of subflares reported [Refs. 25,26], produced frequency variations.

6. Two Solar Flares: The less important One Followed by More Severe Absorption The effects on WWV-20, PR-18, and PR-15 signals by two solar flares of 4 September 1961 are depicted in Fig. 8. In both cases the frequency variations vary inversely with operating frequency. Absorption also sets in but reaches its maximum value about 4 min after the maximum frequency variations. A very small, almost undistinguishable, deviation toward the south of the 15-Mc angle of arrival can be observed during the time of the first flare-induced frequency change. Notice that the absorption effect is more severe and lasts longer for the case of less importance (importance 1).

7. Two Solar Flares of Importance 1 Inducing Widespread Changes. Figure 9 shows another example of two solar flares of 13 August 1961 of reportedly equal importance (1), yet producing completely different results. The first produced noticeable frequency changes and substantial absorption (almost simultaneously with the time interval of frequency change and angle-of-arrival deviations to the south). The second produced no readily noticeable changes in frequency and almost no absorption. An angle-of-arrival deviation to the south about 6 min prior to the maximum phase of the second flare is noticed on the 15-Mc signal (see arrow on the 15-Mc angle-of-arrival channel). Thus, it is evident that even though the visual observation of two flares seems identical, their ultra-violet and X-ray energy releases could be different as indicated by their substantially different effects on the ionosphere that affects h-f waves passing through it.

8. Solar Flare Inducing Frequency Changes but no Absorption. Figure 10 shows another effect of a solar flare on 29 July 1961 that produced frequency changes but no absorption. The intensification of the

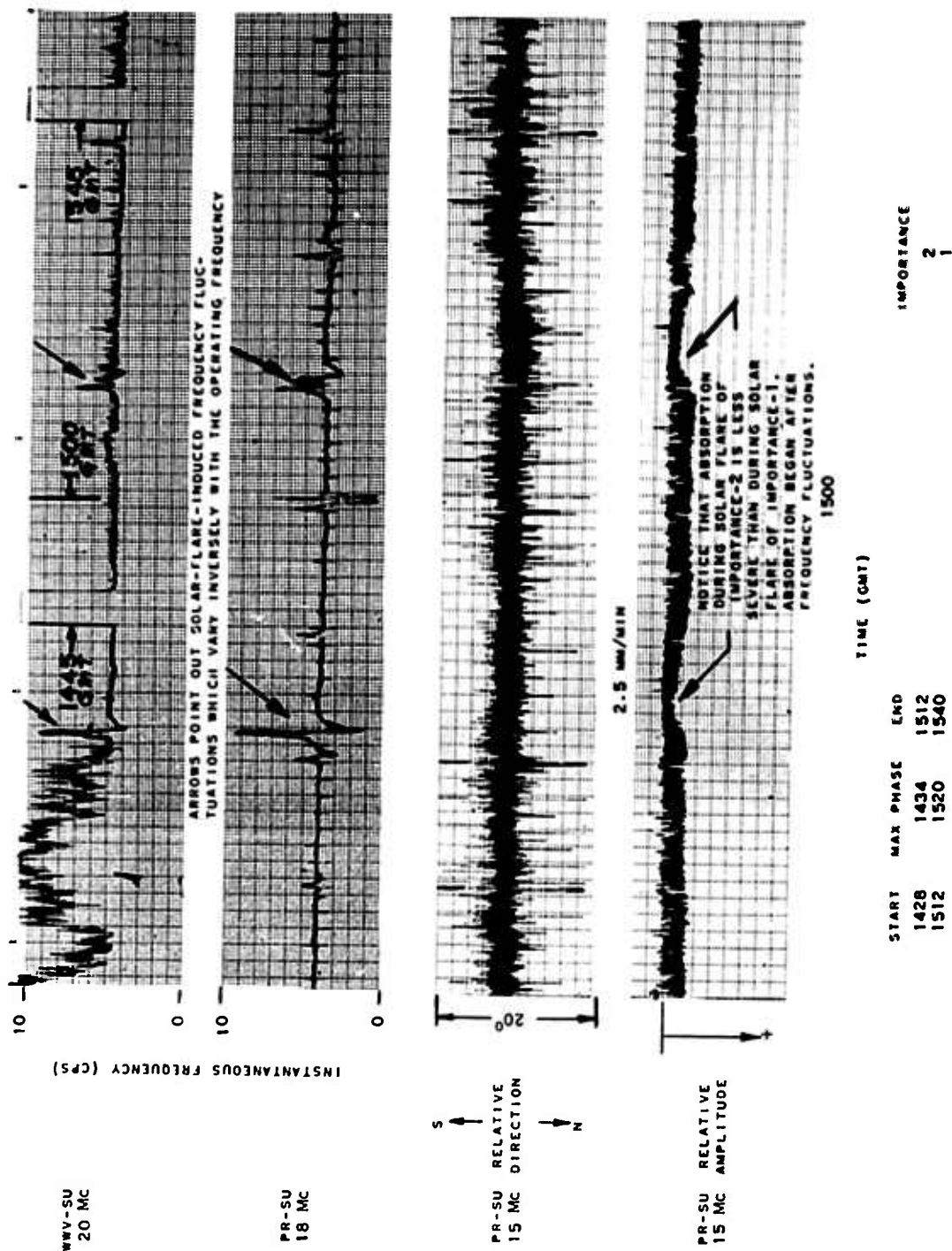


FIG. 8. EXAMPLES OF TWO SOLAR FLARES OF 4 SEPTEMBER 1961. THE LESS IMPORTANT ONE FOLLOWED BY MORE SEVERE ABSORPTION.

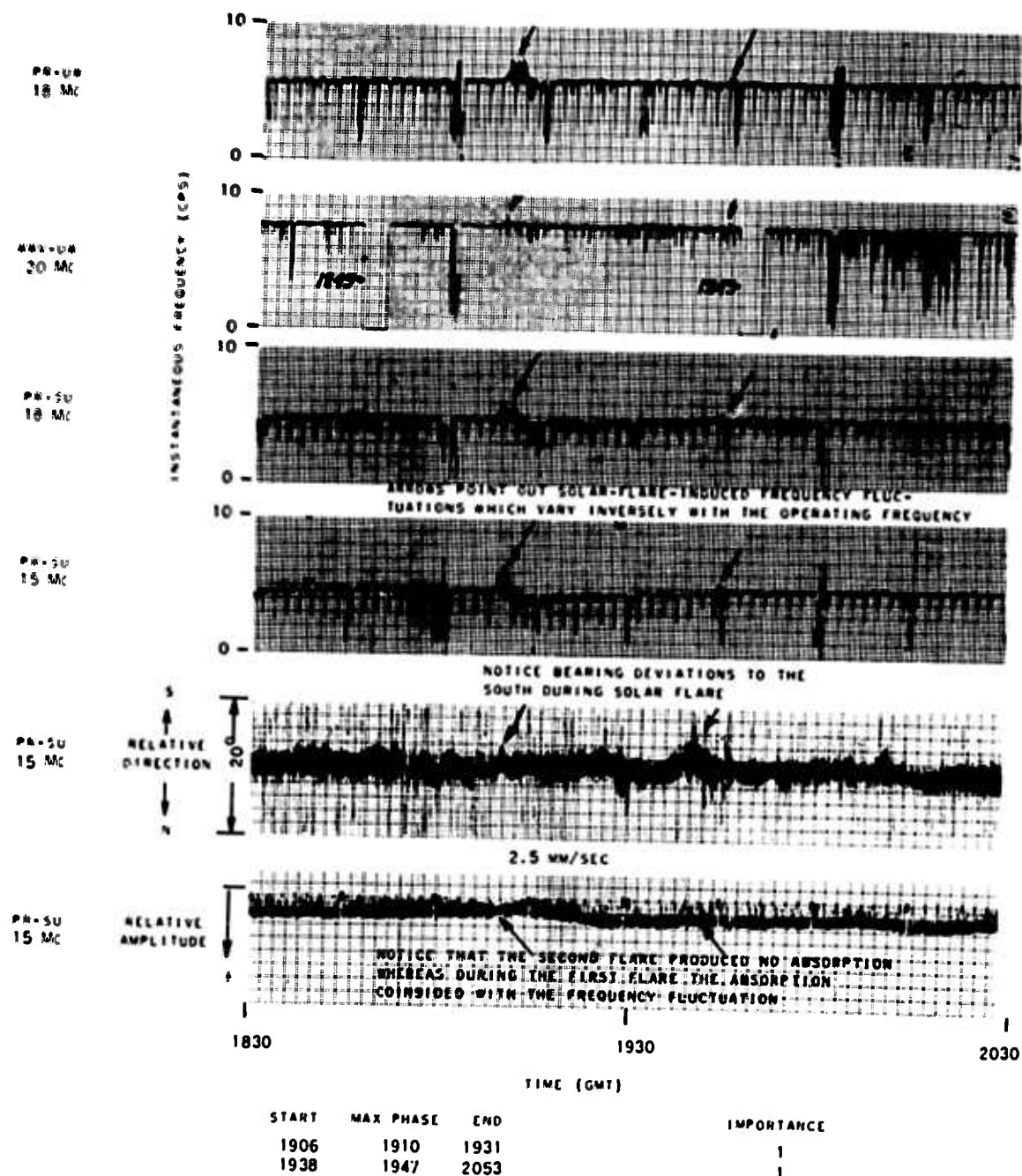


FIG. 9. TWO SOLAR FLARES OF IMPORTANCE 1 INDUCING WIDESPREAD, AND DIFFERENT, FREQUENCY AND BEARING CHANGES, 13 AUGUST 1961.

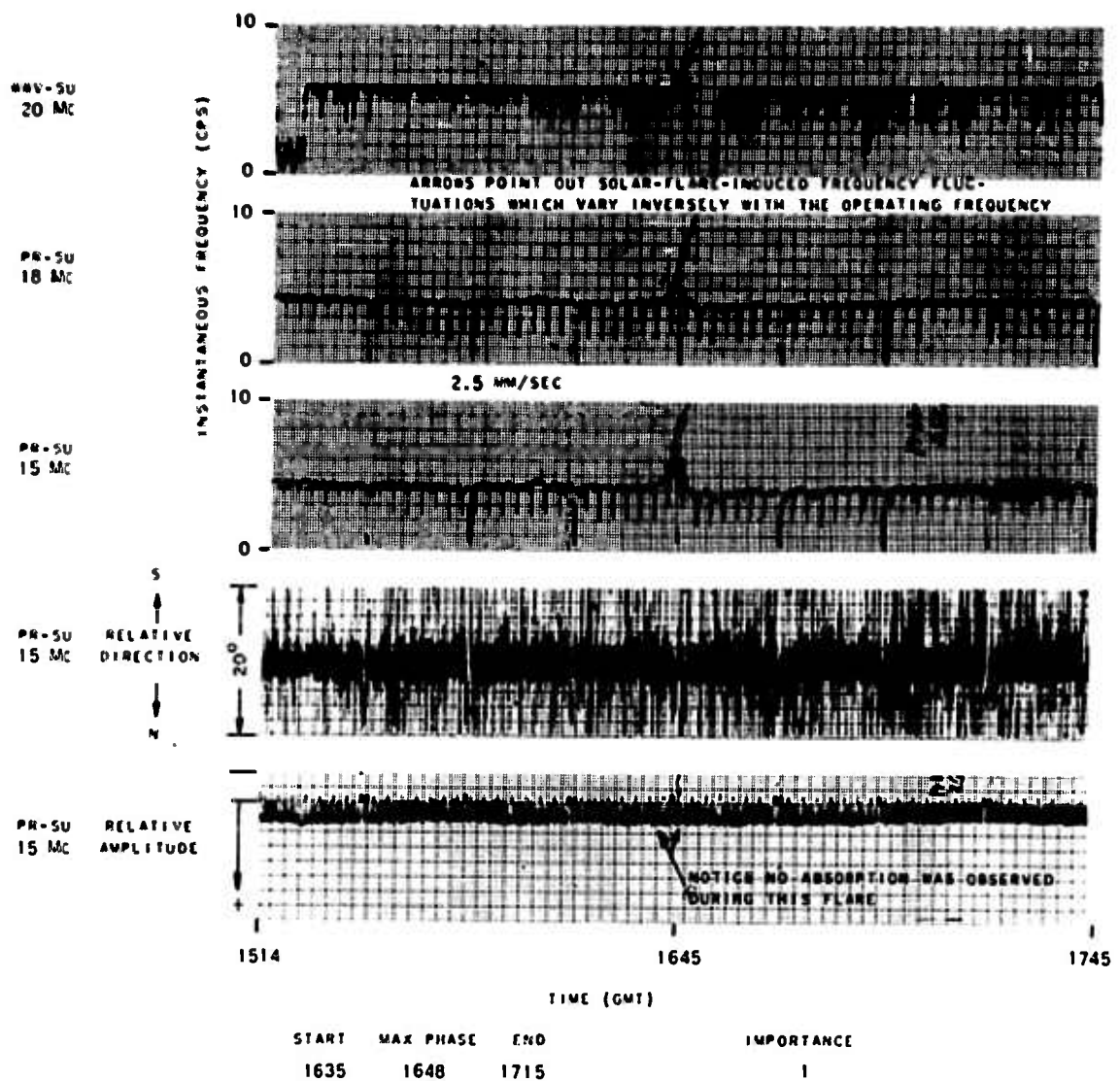


FIG. 10. EXAMPLE OF SOLAR-FLARE INDUCED FREQUENCY CHANGES BUT NO ABSORPTION.

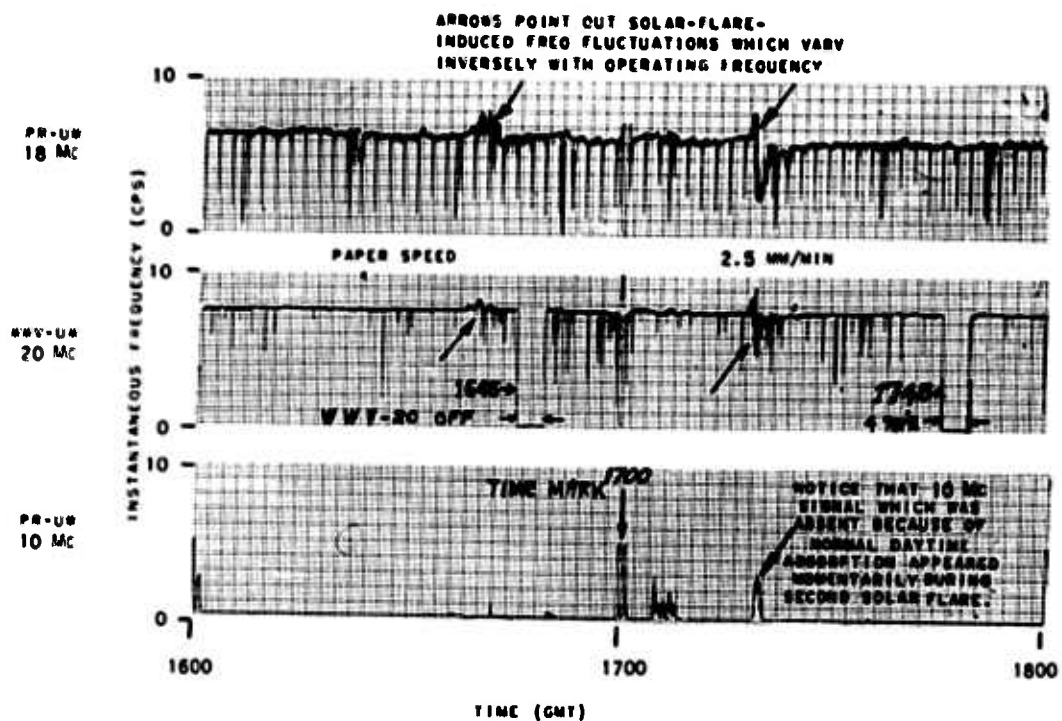
bearing scintillations on the 15-Mc signal following the solar flare is evident in this case, but angle-of-arrival deviations are not produced. Notice again that the frequency variations vary inversely with the operating frequency.

9. Signal Enhancement During the Solar-Flare Maximum Phase.

Figure 11 is an example of the appearance of a signal which had been normally absent because of daytime absorption. Notice that the 10-Mc signal (PR-UW), weak because of normal daytime absorption, came in momentarily stronger during the second flare (see arrow in third--bottom--channel). Such enhancements of signals during solar flares have been reported also by others [Ref. 21].

10. Short-Lived Azimuthal Bearing During Solar Flare. Figure 12 shows more clearly the effect of a solar flare on 29 July 1961 on the angle of arrival. At the time of the frequency deviation, the angle of arrival of the 15-Mc signal had been shifted south of its previous bearing by about 3 deg. In this figure the frequency shifts also vary inversely with the operating frequency. This is also an example of an enhancement rather than an attenuation of the amplitude of the 15-Mc signal following the solar flare.

11. Simultaneous Absolute Phase and Amplitude Rapid-Run Records of Solar-Induced Changes. Figure 13 shows simultaneous phase and amplitude rapid-run recordings of the PR-18 and PR-15 transmissions received at SU on 28 September 1961. This example is one which shows some of the most severe effects on the amplitude and phase of h-f signals recorded during the 2-month recording period. Because of its detailed and prolonged occurrence, this effect will be analyzed more fully later (see Chapter IV). Suffice it to say that the net phase changes for the 18- and 15-Mc signals were 1200 and 1400 cycles, respectively, over the background presolar value and that no amplitude reduction was set in during the positive phase of the solar flare (while the phase was increasing with time). The absorption started to set in just prior to the time of the maximum phase change. It is also emphasized here that the phase change is very close to $1/f$ ($\frac{1200}{1400} \approx \frac{15.1}{17.9}$). Also, the recovery of the flare-induced phase change lasted many minutes beyond the recovery of the



START	MAX PHASE	END	IMPORTANCE
1629	1633	1727	1+
1629	1643	1727	1+
1630	1642	1723	2
1718	1720	1728	1
1717	1718	1730	1+

FIG. 11. EXAMPLE OF SIGNAL ENHANCEMENT DURING SOLAR-FLARE MAXIMUM PHASE, 15 JUNE 1961.

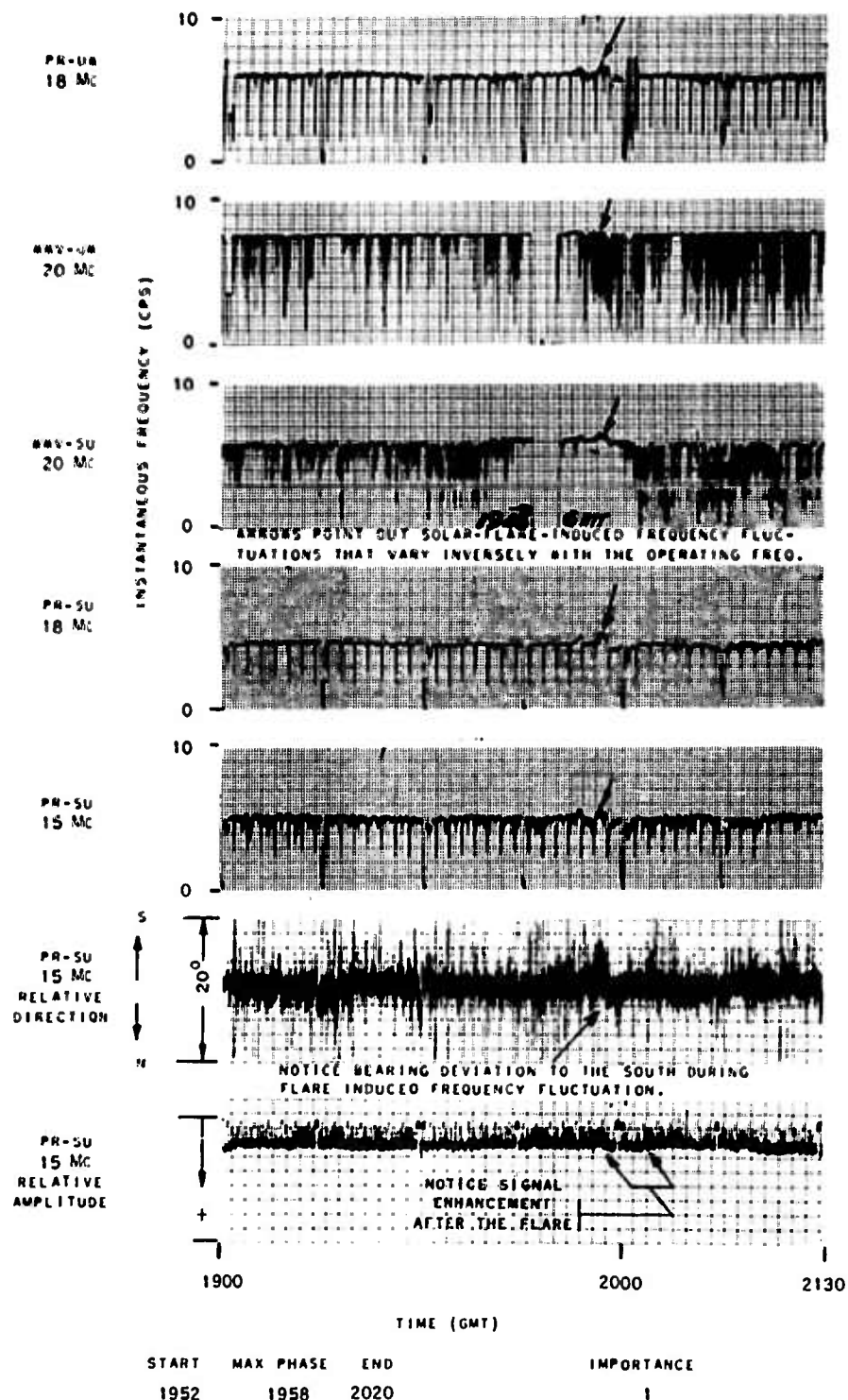


FIG. 12. EXAMPLE OF SHORT-LIVED AZIMUTHAL-BEARING CHANGE DURING SOLAR FLARE, 29 JULY 1961, SHOWING EFFECTS ON WIDELY SEPARATED SIGNAL PATHS.

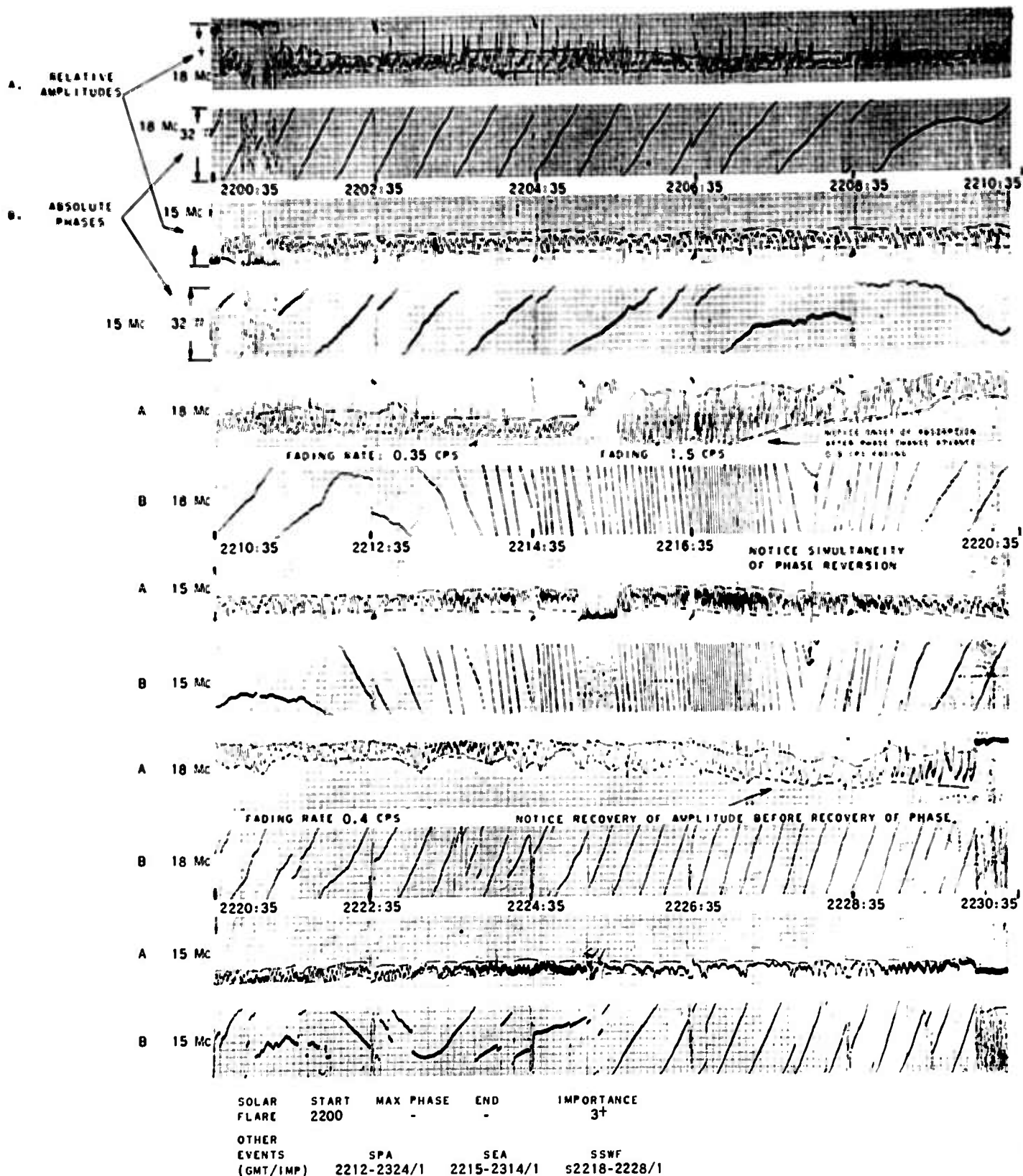


FIG. 13. SIMULTANEOUS PHASE AND AMPLITUDE RAPID-RUN RECORDS SHOWING DETAILED CHANGES INDUCED DURING SOLAR FLARE OF IMPORTANCE 3+, 28 SEPTEMBER 1961.

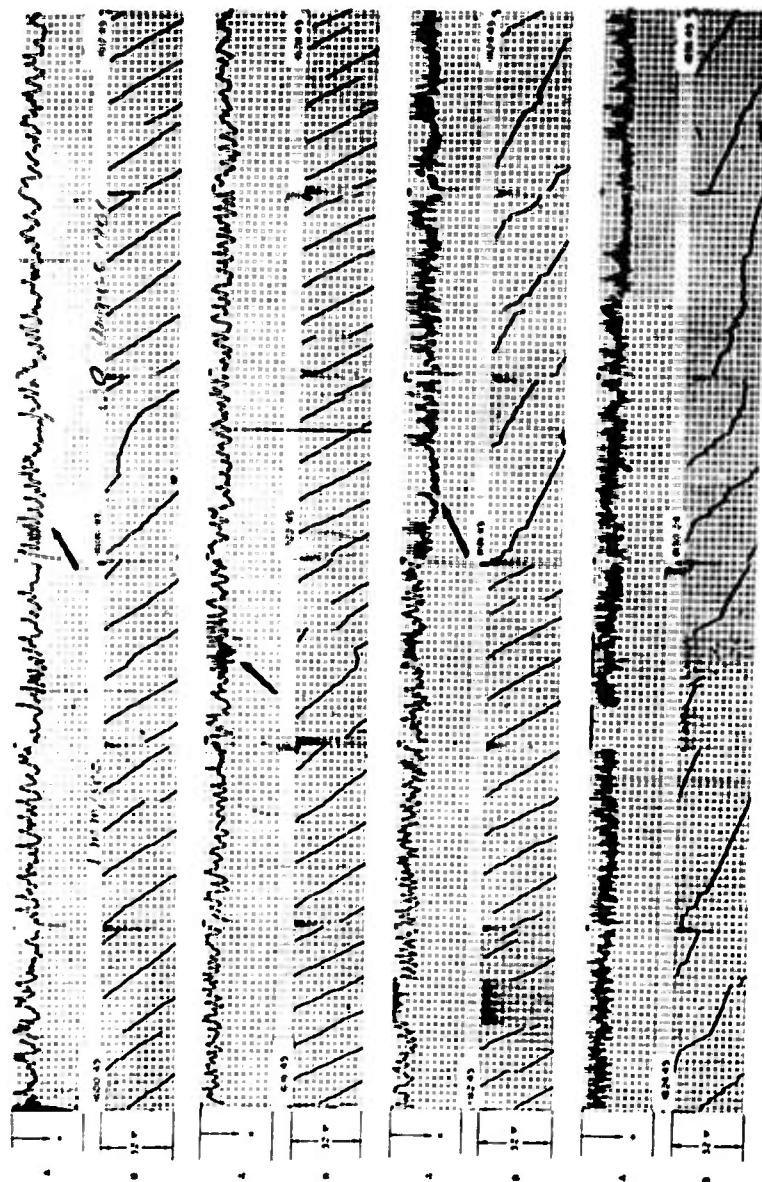
signal due to absorption, thus indicating that the ionization changes that produce the absorption and frequency changes are of different origin and at different levels.

As a final comment concerning the effect of the solar flare shown in Fig. 13, observe that for both frequencies the maximum phase is reached at the same time to within ± 0.5 sec. The time coincidence indicates that both the 15- and 18-Mc wave transmissions were affected simultaneously. Since each one is refracted at a different height of the ionosphere, there could not be a layer moving down because of the simultaneity. Since there was no absorption, the ionization needed to change the phase could not be in the lower ionospheric layers (i.e., D or E). Thus, most ionization changes must have taken place in a narrowband between the E and F layers. This layer will be shown to lie somewhere between 120 and 160 km in height (see Chapter IV).

12. Absolute Phase and Amplitude Rapid-Run Records Depicting Solar-Flare and Subflare-Induced Effects. All solar flares do not produce severe, almost spectacular results such as those shown in Fig. 13. One sometimes has to hunt through the records with previous knowledge of solar-flare events to find any effects (see, for example, Figs. 14 and 15). Notice the increase in the fading rate of the amplitude during the phase changes at about 1607, 1621, 1819, and 1824 to 1836 of Fig. 14 (arrows). The phase changes during the maximum phases of the subflares at about 1612, 1625, and 2007 are also evident in Fig. 15.

C. SPECTRUM ANALYSIS OF SHORT-PERIOD FREQUENCY FLUCTUATIONS

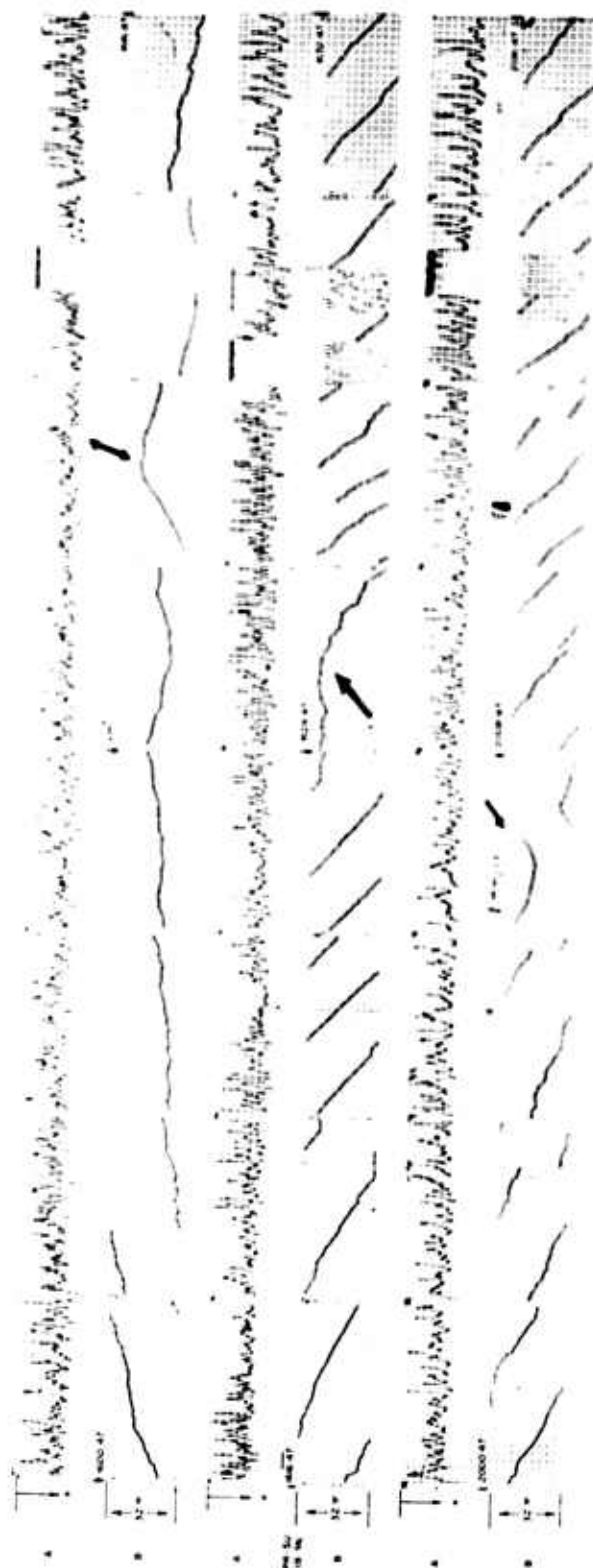
As shown in the previous examples, particularly in Figs. 9 and 12, the solar-flare-induced effects are widespread. Thus, traveling disturbances must be excluded since, if they were isolated, they could not travel fast enough to affect all of the paths simultaneously. One should distinguish, however, two main kinds of short-period frequency fluctuations: those produced by solar-flare-induced ionization which vary inversely with the operating frequency, and those produced by sudden geomagnetic-field fluctuations (i.e., sudden commencements) which most often vary proportionally with the operating frequency. The first



CHANNEL A: RELATIVE AMPLITUDES CHANNEL B: RELATIVE AMPLITUDES
ARROWS POINT OUT INCREASED FADING RATE AT THE TIME OF SOLAR-FLARE-INDUCED PHASE CHANGE.

START	MAX PHASE	END	IMPORTANCE
1552	-	1630	1
BEFORE 1623	-	AFTER 1647	1

FIG. 14. EFFECTS OF SOLAR FLARES ON PHASE AND AMPLITUDE OF 18-Mc PR-SU SIGNAL. 30 AUGUST 1961.



ARROWS POINT OUT THE SOLAR-FLARE-INDUCED PHASE
REVERSALS DURING WHICH THE FADING RATE WAS
INCREASED.

CHANNEL A: RELATIVE AMPLITUDES		CHANNEL B: ABSOLUTE PHASES	
START	MAX PHASE	END	IMPORTANCE
(A) 1608	1612	1618	1-
(B) 1625	1625	1644	1-
(C) 2006	2009	2021	1-

FIG. 15. EFFECTS OF SOLAR SUBFLARES ON PHASE AND AMPLITUDE OF 18-Mc PH-SU
SIGNAL, 25 AUGUST 1961.

kind of frequency fluctuation affects all propagating modes, including those of the ordinary and extraordinary waves, by roughly the same amount. During the second kind of fluctuation, the many propagating modes over the same path are affected by slightly different amounts. Thus, when frequency is analyzed, the incoming spectrum is split on the record.

Solar flares affect only the signals which propagate in the sunlit part of the earth, whereas sudden commencements can affect the h-f transmission at either day or night. Even though the sudden commencements occur less frequently than the solar flares (three to four each month, on the average, as compared with two to three solar flares a day), their effect on the instantaneous frequency is noticed as much on the records as those of solar flares, since 90 percent of sudden commencements produce frequency changes as compared with about 20 percent of solar flares.

1. Solar-Flare-Induced Fluctuation--No Mode Frequency Splitting.

Figure 16 shows a frequency analysis of the received-frequency spectrum of a solar-flare-induced frequency fluctuation. It is clearly seen that the many existing modes previous to the solar flare constitute a frequency band about 1 cps wide. During the solar-flare maximum, the whole band of frequencies is affected by the same amount.

2. Fluctuation Caused by a Sudden Commencement--Mode Frequency Splitting Figure 17 shows an analysis of the received-frequency spectrum of short-lived frequency variations that took place during a sudden commencement that resembles those produced by solar-flare-induced ionization (i.e., a slight increase in the frequency followed by a decrease and a subsequent recovery). During the sudden increase in the geomagnetic field the frequency increased; then, when the magnetic field suddenly decreased, the frequency also decreased. Notice, however, that the many different frequencies coming in prior to the geomagnetic fluctuations with a bandwidth of about 1 cps, are affected differently and "frequency splitting" on the record occurs, a characteristic that is not observed during the solar-flare-induced fluctuations.

3. Fluctuation During a Large Geomagnetic-Field--Mode Frequency Splitting and Continued Frequency Oscillations. Another characteristic

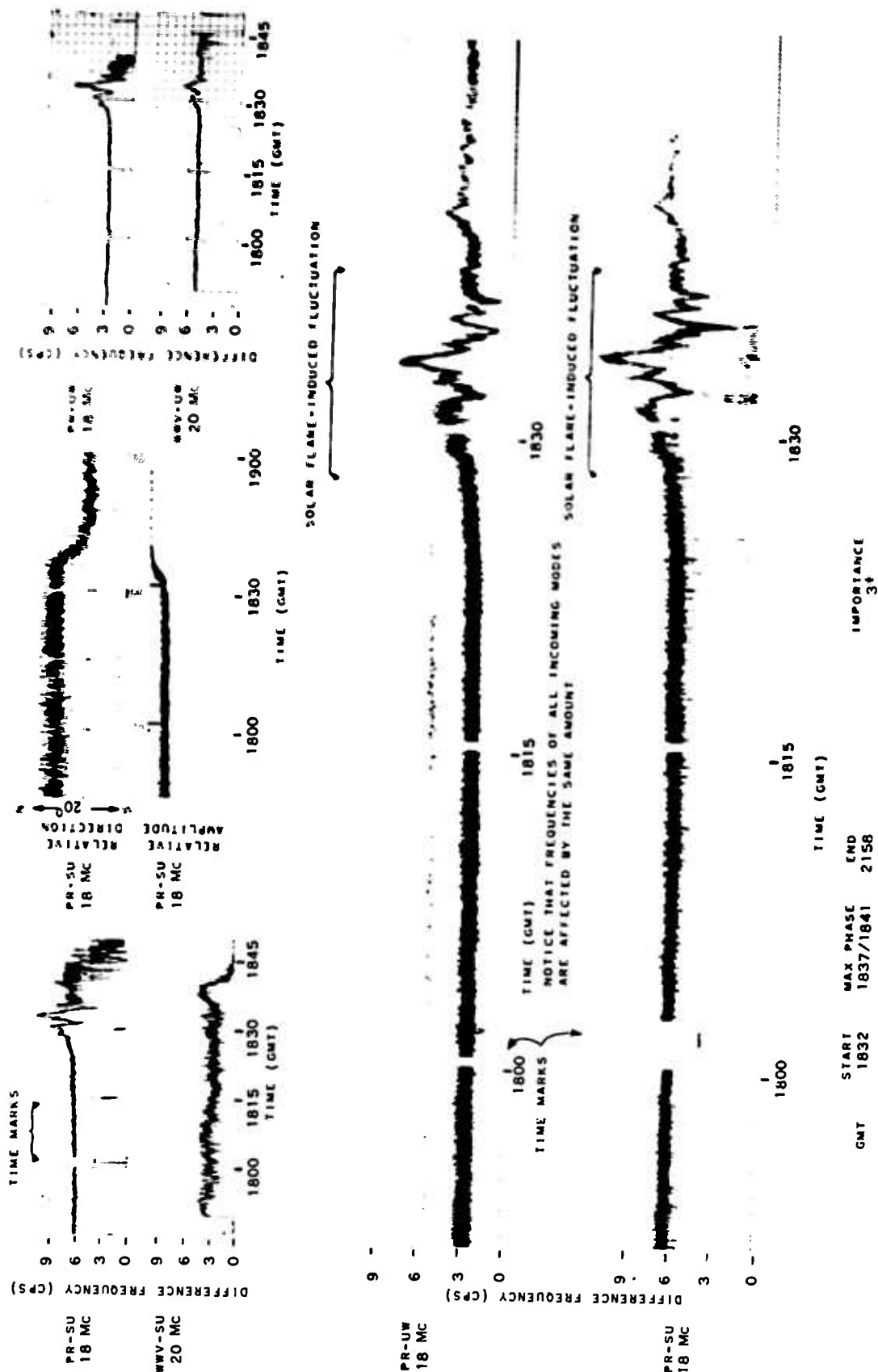


FIG. 16. FREQUENCY ANALYSIS OF TOTAL RECEIVED FREQUENCY SPECTRUM OF SOLAR-FLARE-INDUCED FREQUENCY FLUCTUATION, 4 DECEMBER 1960. FREQUENCIES OF ALL INCOMING MODES AFFECTED BY SAME AMOUNT.

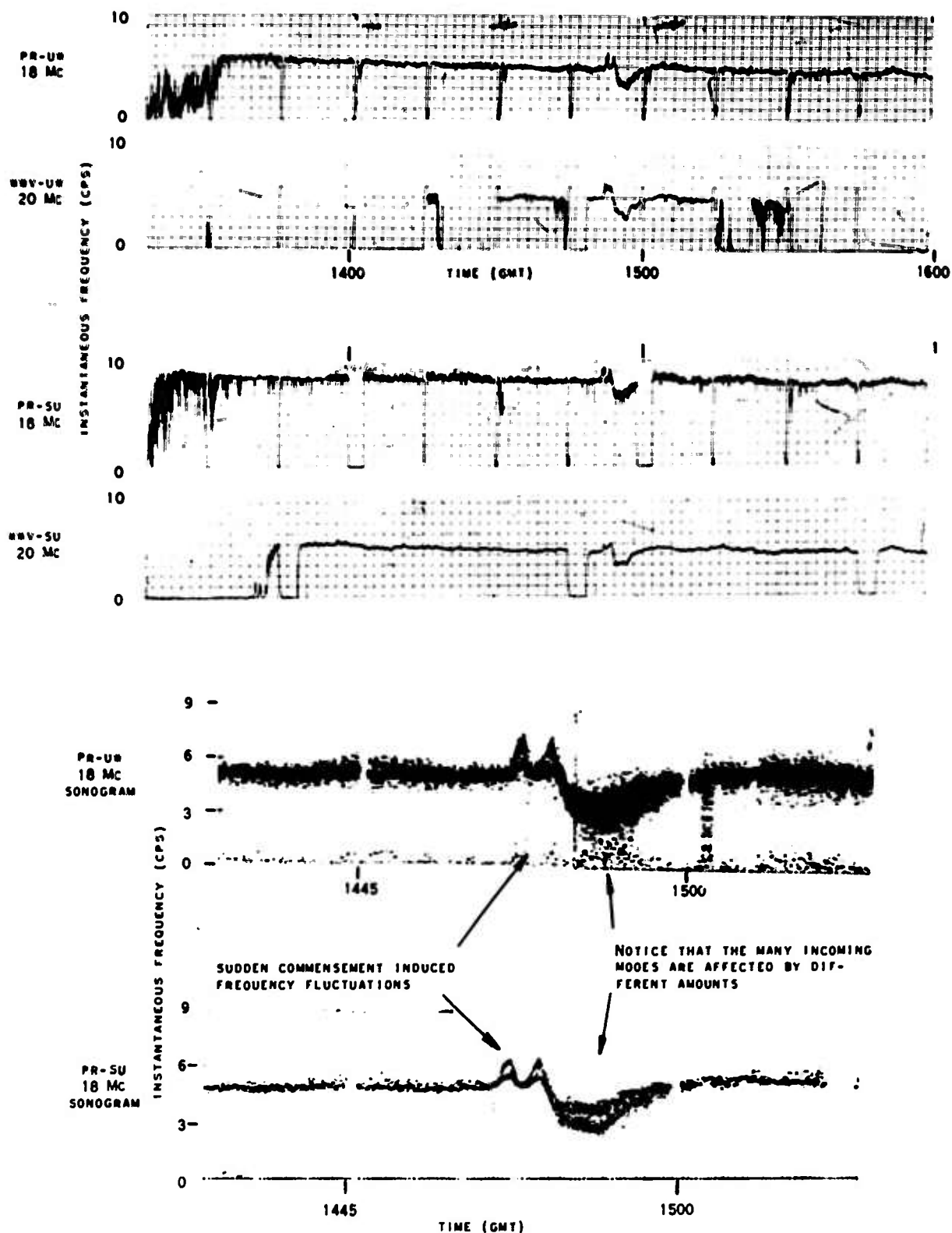


FIG. 17. FREQUENCY ANALYSIS OF TOTAL RECEIVED FREQUENCY SPECTRUM OF FREQUENCY FLUCTUATION CAUSED BY SC, 24 OCTOBER 1961. FREQUENCIES OF THE MANY INCOMING MODES AFFECTED BY DIFFERENT AMOUNTS.

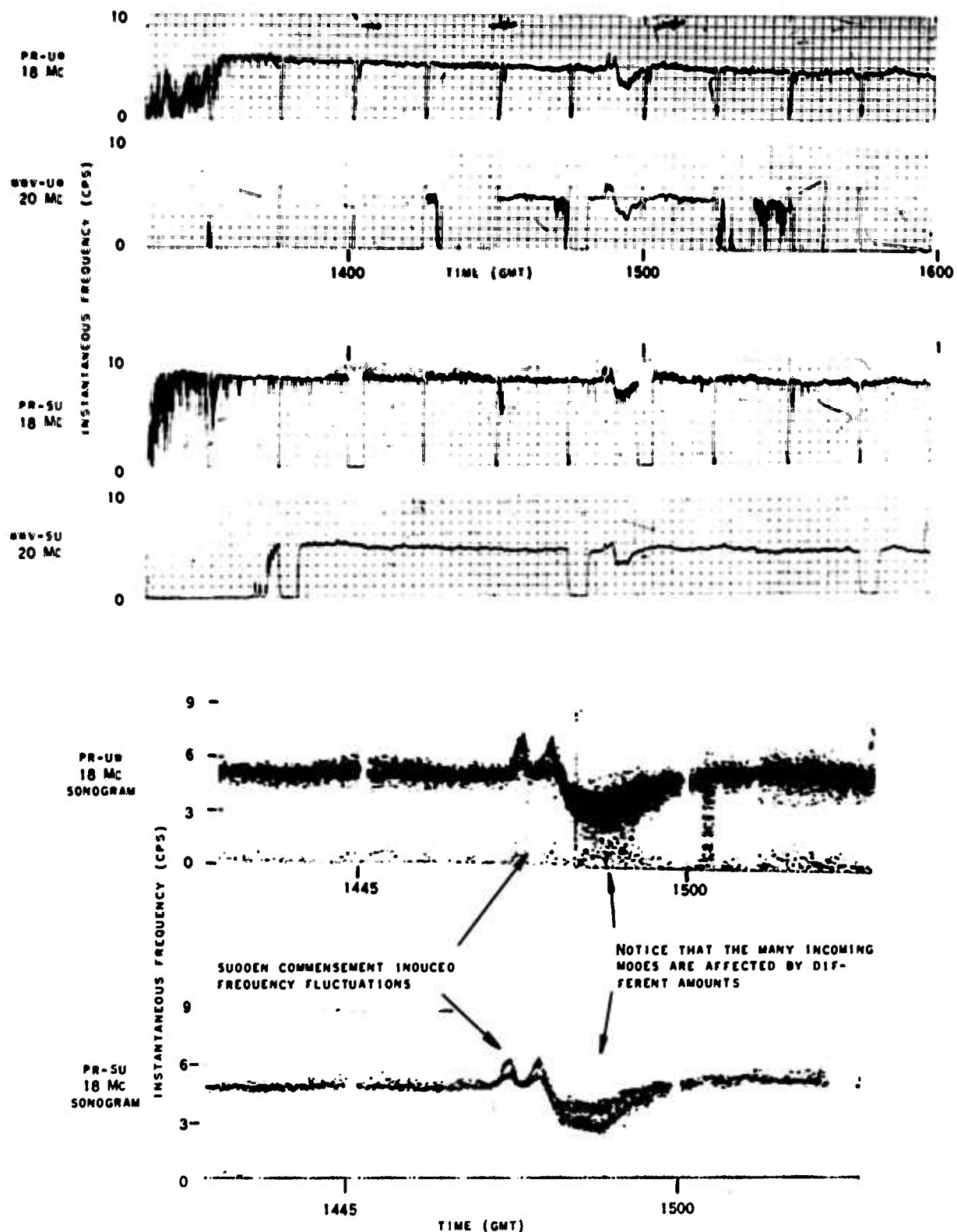


FIG. 17. FREQUENCY ANALYSIS OF TOTAL RECEIVED FREQUENCY SPECTRUM OF FREQUENCY FLUCTUATION CAUSED BY SC, 24 OCTOBER 1961. FREQUENCIES OF THE MANY INCOMING MODES AFFECTED BY DIFFERENT AMOUNTS.

of the short-period fluctuations that is observed during the sudden geomagnetic-field fluctuations but not during the solar-flare-induced frequency fluctuations, is the following: the short-lived frequency fluctuations, which usually vary proportionally with the operating frequency, continue for a long time after the sudden geomagnetic-field variation, as shown in Fig. 18. Notice that the frequency decrease of the 10-Mc PR-SU signal is about 3 cps, whereas that of the 20-Mc WWV-SU signal is about 6 cps, a 2 to 1 variation. In the same figure observe that the 15-Mc angle of arrival shifted toward the south by about 2 deg while the frequency was decreasing. The angle of arrival of the 10-Mc PR-SU signal did not deviate during this frequency variation, but the bearing scintillations increased in amplitude markedly after it. In this case the vertical angle changed much more than the azimuthal angle of arrival because of a probable vertical movement of the ionospheric layer. The equipment, however, is not sensitive to the vertical angle-of-arrival changes.

4. Fluctuation Caused by a Sudden Impulse--Mode Frequency Splitting Occurring Simultaneously over Widely Separated Paths. Figure 19 shows another example of a short-lived frequency change that correlates with the simultaneous occurrence of a rapid geomagnetic-field variation (magnetic sudden impulse) that took place on 4 February 1961. The magnetic field suddenly increased by about 15 gamma* at 1828, then decreased by more than 40 gamma at about 1830. The frequency splitting and subsequent "ringing" of the frequency are present in this case also. Notice that the frequency of the 20-Mc signal varied more than that of the 15-Mc during the time interval under discussion. The fact that the azimuthal angle of arrival is not affected drastically during these sudden geomagnetic-field variations could be due to a vertical movement of the refraction point of the wave (see the proportional frequency variation of the instantaneous frequency and the simultaneous effect on widely separated paths). Subsequent motions of the ionosphere, however, could produce tilts that would deviate the h-f waves laterally [Ref. 24]. In other words, the upper layers of the ionosphere can be considered as a filter which "rings" whenever energy is applied to it.

*1 gamma = 10^{-5} gauss

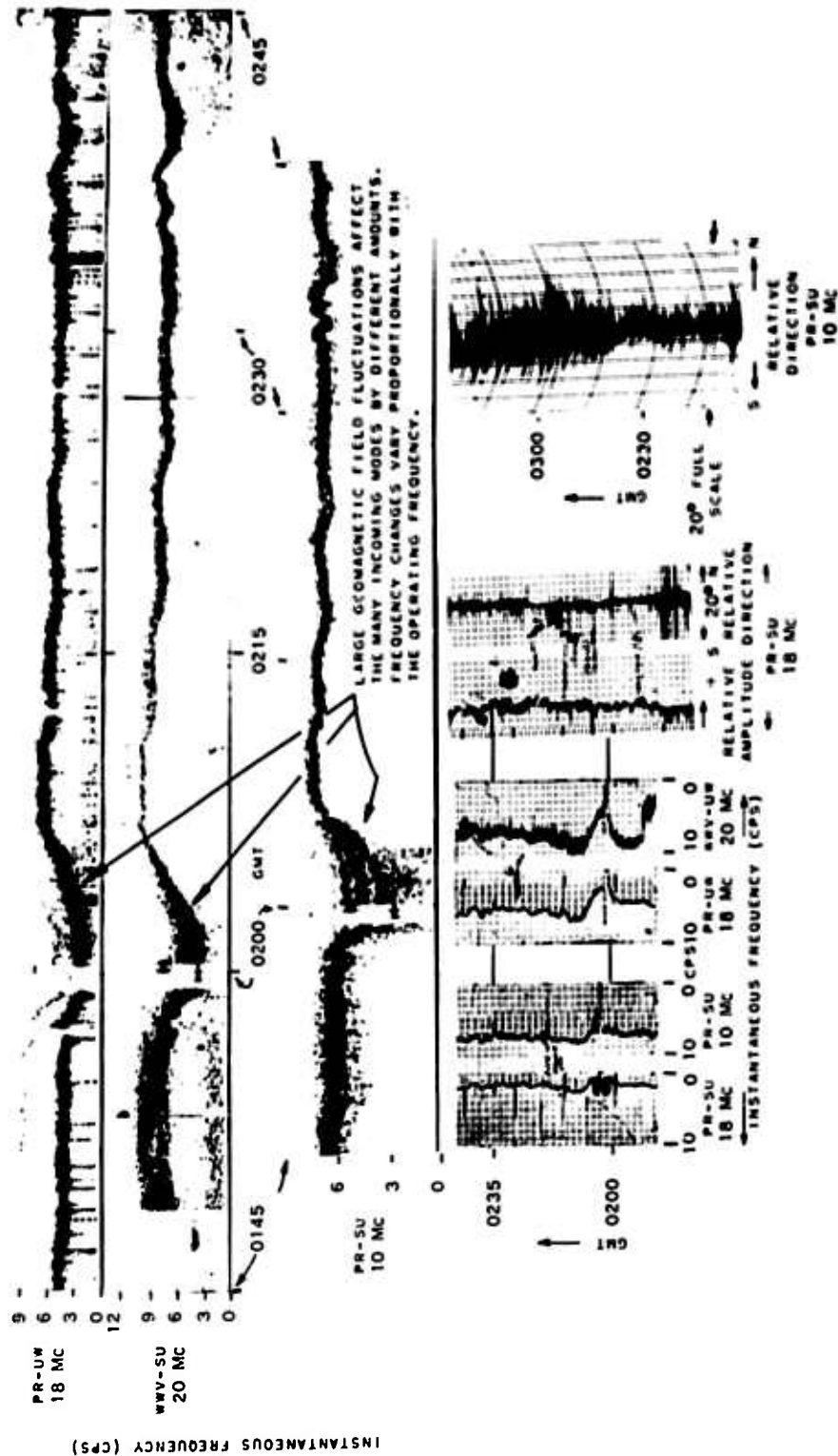


FIG. 18. FREQUENCY ANALYSIS OF TOTAL RECEIVED FREQUENCY SPECTRUM OF FREQUENCY FLUCTUATION DURING LARGE GEOMAGNETIC-FIELD FLUCTUATION, 28 MARCH 1961. FREQUENCIES OF THE MANY INCOMING MODES AFFECTED BY DIFFERENT AMOUNTS, CONTINUING FREQUENCY OSCILLATIONS.

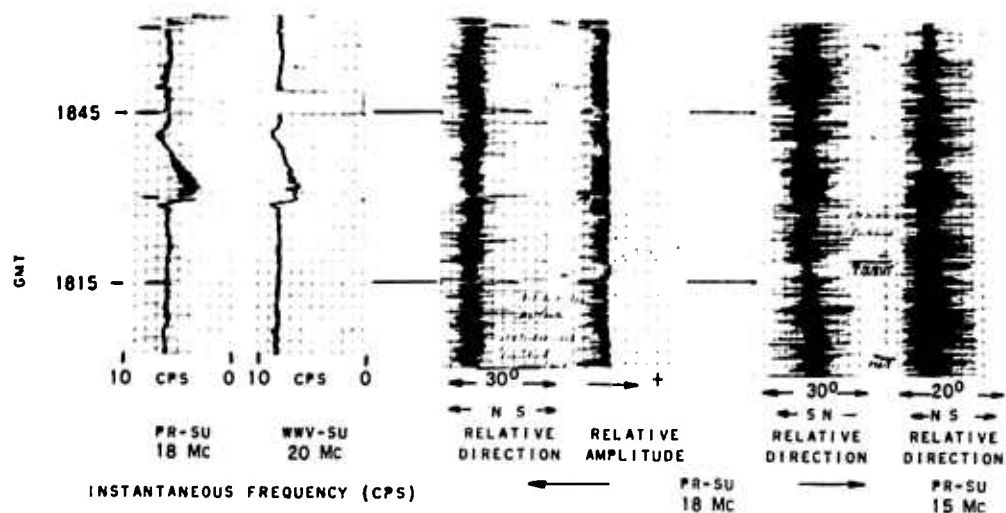
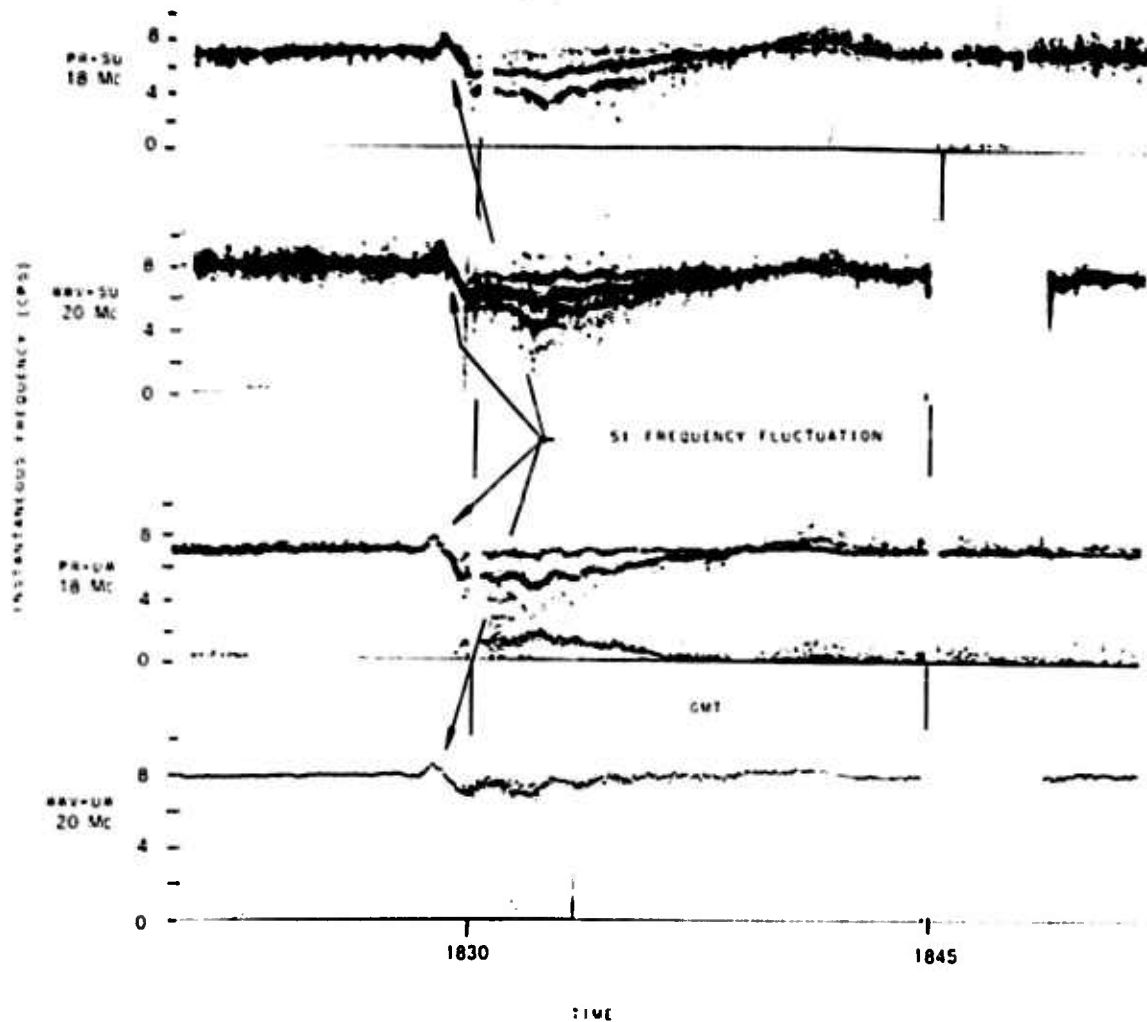


FIG. 19. FREQUENCY ANALYSIS OF TOTAL RECEIVED FREQUENCY SPECTRUM OF FREQUENCY FLUCTUATION CAUSED BY SI, 4 FEBRUARY 1961. FREQUENCIES OF THE MANY INCOMING MODES AFFECTED BY DIFFERENT AMOUNTS SIMULTANEOUSLY OVER WIDELY SEPARATED PATHS.

IV. THEORETICAL CONSIDERATIONS AND EXPERIMENTAL ANALYSIS

The experimental observations discussed in Chapter III can be summarized as follows:

1. All solar flares of the same class do not produce similar effects. Sometimes there can be a 2 to 1 difference in the amount of frequency change, and time intervals of their effects can range from 1 to 5 min.
2. Some flares (even of importance 2, 3, or 3+) do not produce any effects.
3. Solar flares are accompanied by short-wave fadeout, others are not. Some flares of the same kind during the same day produce different changes. The short-wave fadeout, when it occurs, takes place after the frequency angle-of-arrival deviations to the south* of the great-circle plane, and it has occurred as many as 2 to 5 min later.
4. The frequency changes vary inversely with operating frequency, as contrasted with the frequency changes which vary proportionally with the operating frequency, because of the reflection point of the h-f wave moving upward or downward.
5. The maxima of the frequency shifts take place 1 to 4 min prior to the time of the maximum phase of the solar flares.
6. The short-lived frequency change produced during solar flares can be distinguished from those produced during sudden geomagnetic-field variations. In the former case all modes are affected by the same amount; whereas, in the latter, frequency splitting and ringing occurs.

In the following sections, simple expressions for the frequency and phase change, as well as for the absorption of ionospherically propagated wave, will be obtained and values for these effects under various ionospheric changes will be calculated. These results will then be compared with experimental observations. It will be shown that the ionization changes in the D region needed to produce the frequency and phase changes reported, would also produce large absorption levels of the propagation signals. From the simultaneity nature of the effects over large areas, and the fact that a wave also deviates off its great-circle plane, as well as from other considerations, it will be shown that

* South of the great-circle plane is not the only direction toward which an h-f wave will deviate. It depends on the relative position of the path to the sun, the season in which the measurements were made, and the frequencies of operation.

solar flares often produce ionization above 125 km but below the points where the h-f waves of the 15- to 20-Mc range are "reflected".

The vlf experiments [Refs. 7,14,19] have shown that the effects of the D region and lower lag the effects of the E region and higher, and this is borne out by the examples shown in the previous chapter. Thus, further evidence is given to support the fact that ionization increase is also produced between the E and F regions by a different ionization agent than that which produces ionization in the D region. Furthermore, the data presented here indicate that all layers (i.e., heights) are not affected simultaneously; radiation arrives and affects the higher regions first, and later the shorter wavelength X-ray radiation, etc., may or may not come to affect the D or lower region.

A. MATHEMATICAL MODEL

The behavior of an h-f wave transmitted through the ionosphere is completely described if its frequency f and its propagation function γ are given. That is, each wave is of the form:

$$\text{Wave} = E_0 \exp \left[j\omega t - \int_T^R \gamma ds \right] = E_0 \exp \left[- \int_T^R \alpha ds \right] \exp \left[j \left(\omega t - \int_T^R \beta ds \right) \right] \quad (1)$$

where

E_0 = amplitude of wave as it leaves transmitter T,

ω = operational angular frequency = $2\pi f$,

$\gamma = \alpha + j\beta$ = propagation function (per/m),

α = the attenuation part of the propagation function (nepers/m),

and β = phase part of the propagation function (radians/m).

Each integral in Eq. (1) is from the transmitter T to the receiver R.

The propagation function, γ , of an h-f wave traveling through the ionosphere is given by the Appleton-Hartree formula [Ref. 27]:

$$\gamma^2 = -\beta_v^2 + \frac{2 \left(\frac{\omega_H}{\omega}\right)^2 \beta_v^2}{2(1 - j \frac{\nu}{\omega}) - \frac{(\frac{\omega_H}{\omega} \sin \theta)^2}{1 - j \frac{\nu}{\omega} - (\frac{\omega_H}{\omega})^2} \pm \sqrt{\left[\frac{(\frac{\omega_H}{\omega} \cos \theta)^2}{1 - j \frac{\nu}{\omega} - (\frac{\omega_H}{\omega})^2} \right]^2 + 4 \left(\frac{\omega_H}{\omega} \cos \theta\right)^2}} \quad (2)$$

where the symbols have their usual significance (see also List of Symbols). The plus sign gives the propagation function of the ordinary wave, and the minus sign that of the extraordinary.

For the geometry at hand the so-called quasi-longitudinal (QL) approximation of Eq. (1) can be used. This takes the form [Ref. 27]

$$\gamma^2 = \beta_v^2 - \beta_v^2 \frac{\left(\frac{\omega_H}{\omega}\right)^2}{1 - j \frac{\nu}{\omega} \pm \frac{\omega_H}{\omega} |\cos \theta|} \quad (3)$$

Since the operating frequency ranges between 15 and 20 Mc and the gyro-frequency is about 1.25 Mc, the term $\omega_H/\omega \cos \theta|_{\theta=60^\circ}$ compared with 1 can be neglected for the purpose of calculating the attenuation.

Thus, for both the ordinary and extraordinary waves, one has

$$\gamma = \frac{\omega}{c} \sqrt{1 - \left(\frac{\omega_H}{\omega}\right)^2 \frac{1}{1 - j \frac{\nu}{\omega}}} = \alpha + j\beta \quad (4)$$

B. FREQUENCY AND PHASE VARIATIONS

For the purpose of calculating phase or frequency changes one may neglect the term ν/ω but keep the term $\omega_H/\omega \cos \theta$ in order to see the effect of the magnetic field. Propagation is controlled by β when $\omega_H < \omega$ but not much smaller than ω_H . Then:

$$\beta = \frac{\omega}{c} \left[1 - \left(\frac{\omega_H}{\omega}\right)^2 \frac{1}{1 \pm \frac{\omega_H}{\omega} |\cos \theta|} \right]^{1/2} \quad \text{when } \frac{\nu}{\omega} \ll 1 \quad (5)$$

Thus, neglecting momentarily the attenuation function, one has for the ordinary mode

$$\text{Wave} \propto \exp \left[j\omega t - j \int_T^R \beta ds \right] = e^{j\vartheta} \quad (6)$$

where ϑ is the total phase of the wave. The time derivative of the total phase is the instantaneous angular frequency

$$\frac{d\vartheta}{dt} = \omega_{\text{inst}} \quad \text{radians/sec} \quad (7)$$

When β does not vary with time, $\omega_{\text{inst}} = \omega$, the operating frequency. If β does vary with time, however,

$$\omega_{\text{inst}} = \frac{d\vartheta}{dt} = \omega - \frac{d}{dt} \int_T^R \beta ds \quad \text{radians/sec} \quad (8)$$

It is the time dependence of the second term of Eq. (8) that modifies the phase and instantaneous-received frequency of h-f waves during solar flares.

Assuming an n-hop propagation path between stations separated by a distance d km, we propose that the absorption and frequency variations are due to a change in the ionization of a layer of thickness a km in the nondeviative part of the path [Ref. 20]. For simplicity, let us assume that β is a constant function of the spatial coordinates (x, y, z) as the wave travels through the thin layer of thickness a . Under this assumption β can be taken out of the integral sign and the value of the integral replaced by the incremental path length ΔS .

$$\Delta S = \frac{2 a n}{\sin \psi_n} \quad \text{meters} \quad (9)$$

where $\psi_n = \arctan \frac{2 n h'}{d}$ is the takeoff angle of the wave, and h' is the virtual height of refraction. For this model, β changes with time only in region II (see Fig. 20); thus

$$\vartheta = \omega t - \frac{\omega}{c} \sqrt{1 - \left(\frac{\omega_N}{\omega}\right)^2} \frac{\omega}{\omega \pm \omega_H |\cos \theta|} \Delta S \quad (10)$$

Since

$$\left(\frac{\omega_{H1}}{\omega}\right)^2 \frac{\omega}{\omega \pm \omega_{H1} \cos \theta} < 1,$$

we neglect higher terms in the expansion of the square root to obtain

$$\phi = \omega t - \frac{\omega}{c} \Delta S + \frac{\omega_{H1}^2}{2\omega c} \left(\frac{\omega}{\omega \pm \omega_{H1} \cos \theta} \right) \Delta S \quad (11)$$

The third term in Eq. (11) is due to the ionosphere and

$$\Delta \phi = \frac{\omega_{H1}}{c} \frac{d\omega_{H1}}{dt} \left(\frac{\Delta S}{\omega \pm \omega_{H1} \cos \theta} \right) \quad (12)$$

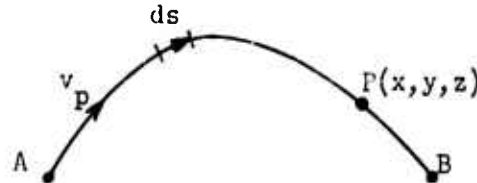
For the frequency case

$$\frac{d\phi}{dt} = \omega + \frac{\omega_{H1}}{c} \frac{\Delta S}{\omega \pm \omega_{H1} \cos \theta} \frac{d\omega_{H1}}{dt} \quad (13)$$

Thus, the frequency and phase of a wave of frequency ω transmitted through the ionosphere vary inversely with the operating frequency when ω_{H1} varies with time in region II.

C. FERMAT'S PRINCIPLE

That the different modes (i.e., ordinary and extraordinary modes of the many n-hop modes) pass through slightly different paths can be seen from Fermat's principle which, for our specific case, states that the integral of the phase path of an electromagnetic wave traveling from a point A (the transmitter) to a point B (the receiver), as shown in the sketch below, is a minimum or

$$\int_A^B \frac{ds}{v_p} = \min$$

(14)

where ds denotes a differential path length transversed by the wave with the phase velocity v_p , but,

$$v_p = \frac{\omega}{\beta} \frac{\text{angular operating frequency}}{\text{propagation function of wave in medium}} \quad (15)$$

Thus, Eq. (14) becomes:

$$\int_A^B \beta \, ds = \min \quad (16)$$

since the operating frequency ω is a constant. In our case the propagation-phase function β is not only a function of the three coordinates (x,y,z) at any point on the path p but of time t as well

Fermat's principle is, of course, subject to certain restrictions, namely, that the propagation function does not have rapid changes (either with space or time) and that the medium is isotropic. These conditions are not met here in a strictly rigorous sense, because the medium is anisotropic and rapid variations in the propagation function are known to take place. Fermat's principle could be used, however, as if the ionosphere were quasi-variable, but the propagation function of the anisotropic medium will be utilized by including the effect of the magnetic field.

In addition to the variations of the propagation-phase function β in the ionosphere, which could affect the ray path of the h-f wave as it travels from A to B, movements or motions of the ionospheric layers modify this path. These motions of the layers produce true doppler-frequency changes in the signal that are proportional to the operating frequency. The frequency variations that take place because of the time variation of the propagation function can be determined by examining the time derivative of the ray path. Thus, the total change in the instantaneous frequency of the wave is given by [Ref. 28],

$$\Delta\omega = \omega \frac{+u_n}{v_p} - \frac{\partial}{\partial t} \int_A^B \beta \, ds \quad (17)$$

or, using Eq. (15),

$$\Delta\omega = \pm u_n \beta - \int_A^B \frac{\partial \beta}{\partial t} \, ds \quad (18)$$

where u_n is the component of the velocity of the moving disturbance along the path. Equation (18) shows that even the doppler-frequency term (a) is affected when the propagation-phase function varies with time. In Eq. (18a) the plus sign is used when the disturbance is moving toward the transmitter, the negative sign when moving away from the transmitter. The negative sign in front of the integral term (b) of Eq. (18) is used because, for the case of forward propagation, the propagation function carries a negative sign, as in Eq. (1).

D. FREQUENCY VARIATIONS WHEN ω_H ONLY VARIES WITH TIME

Examination of the propagation-phase function β of the ordinary and extraordinary waves when ω_H only varies with time, below the height of their refraction points, such as during the sudden introduction of ionization along the ray path, reveals that the time-varying propagation function contributes to a change in the instantaneous frequency. Thus, as the wave advances ΔS meters along its phase path, its instantaneous frequency changes from ω to $\omega + \Delta\omega$. From Eqs. (10) and (11) this change would be proportional to $d\beta/dt$, or

$$\Delta\omega|_{\text{ord}} = \frac{\beta_v^2}{\beta} \frac{\omega_H}{\omega} \frac{\Delta S}{\omega + \omega_H |\cos \theta|} \quad (19)$$

for the ordinary wave, and

$$\Delta\omega|_{\text{extr}} = \frac{\beta_v^2}{\beta} \frac{\omega_H}{\omega} \frac{\Delta S}{\omega - \omega_H |\cos \theta|} \quad (20)$$

for the extraordinary wave.

Since, during the positive part of the phase where ω_H increases, $d\omega_H/dt > 0$ and $\omega_H/\omega \cos \theta \ll 1$,

$$\frac{1}{1 \pm \frac{\omega_H}{\omega} |\cos \theta|} \approx 1 \pm (\omega_H/\omega) |\cos \theta| \quad (21)$$

and there is an increase in the instantaneous frequency of the propagating signal that is proportional to the reciprocal of the operating frequency of the transmitted wave. Furthermore, during electron-density fluctuations:

$$\Delta\omega_{\text{ord}} < \Delta\omega_{\text{extr}} \quad (22)$$

as can be seen by comparison of Eqs. (19) and (20) with Eq. (21). Thus, the ordinary and extraordinary modes are affected differently by the amount $2(\omega_{\text{H}}/\omega \cos \theta)$, since one is decreased by $\omega_{\text{H}}/\omega \cos \theta$ and the other is increased by $\omega_{\text{H}}/\omega \cos \theta$. This difference is small, however, since for the frequencies used here $2 \omega_{\text{H}}/\omega \cos \theta = 2(1.25/17.9) \cos 60^\circ = 0.07$, or the two frequencies differ by only 7 percent in the 17.8825 frequency case. This percentage will increase as the operating frequency approaches the gyrofrequency.

B. FREQUENCY VARIATIONS WHEN ω_{H} ONLY VARIES WITH TIME

With the assumption that ω_{H} varies with time and ω_{H} stays constant, the frequency changes will be proportional to

$$\Delta\omega|_{\text{ord}} = \frac{d\beta}{dt}|_{\text{ord}} = \frac{\beta_v^2}{2\beta} \left(\frac{\omega_{\text{H}}}{\omega}\right)^2 \omega \cos \theta \frac{\frac{d\omega_{\text{H}}}{dt} \Delta S}{(\omega + \omega_{\text{H}} |\cos \theta|)^2} \quad (23)$$

and the frequency of the ordinary mode increases, whereas

$$\Delta\omega|_{\text{extr}} = \frac{d\beta}{dt}|_{\text{extr}} = - \frac{\beta_v^2}{2\beta} \left(\frac{\omega_{\text{H}}}{\omega}\right)^2 \omega \cos \theta \frac{\frac{d\omega_{\text{H}}}{dt} \Delta S}{(\omega - \omega_{\text{H}} |\cos \theta|)^2} \quad (24)$$

and the frequency of the extraordinary mode decreases. In this case again, the many modes are affected differently. The changes in the instantaneous frequency during rapid magnetic changes are inversely proportional to the square of the operating frequency in the nondeviative region where $\beta \ll 1$ (region II of Fig. 20). Close to the point of refraction, however, where $\beta \approx 0$ (region I of Fig. 20), the result is to change the height at which the wave is refracted. The frequency change, then, is proportional to the time derivative of the virtual height; that is, the doppler-type frequency change observed is directly proportional to the operating frequency.

The above statement can be clarified by examining the doppler-frequency change $\Delta\omega$, which is given by

$$\Delta\omega = \omega \frac{d}{dt} \int_T^R \frac{ds}{v_g} \quad (25)$$

where v_g is the group velocity of the wave along the path ds from the transmitter T to the receiver R . Since $v_g = cn$, where c is the velocity of light and n the refractive index in the ionosphere, one has

$$\Delta\omega = \frac{\omega}{c} \frac{d}{dt} \int_T^R \frac{ds}{\sqrt{1 - \left(\frac{\omega_H}{\omega}\right)^2} \frac{\omega}{\omega \pm \omega_H |\cos \theta|}} \quad (26)$$

but $ds \sin \psi_n = dz$, where dz is the vertical-height increment corresponding to the slant incremental path ds , and ψ_n is the takeoff angle of the n th mode. Thus, Eq. (26) can be transformed to

$$\Delta\omega = \frac{\omega}{c} \frac{d}{dt} 2n \sin \psi_n \int_0^h \frac{dz}{\sqrt{1 - \left(\frac{\omega_H}{\omega}\right)^2} \frac{\omega}{\omega \pm \omega_H |\cos \theta|}} \quad (27)$$

or

$$\Delta\omega = \frac{\omega}{c} 2n \sin \psi_n \frac{d}{dt} h' \quad (28)$$

where h' is the virtual height of refraction.

Thus, when the reflecting layer changes height with time, having a component of velocity u_n along the direction of propagation, the second term of Eq. (18) is reduced to a similar expression like the first and a doppler-type of frequency shift is produced which varies proportionally to the operating frequency. The effect of the magnetic field is to cause the ordinary and extraordinary modes to be refracted from different heights in the ionosphere. Therefore, h' varies differently for the ordinary case (plus sign in Eq. 28) than for the extraordinary case (minus sign in Eq. 28). The result is a splitting, on the record, of the frequency spectrum of the incoming transmission.

F. CALCULATIONS OF ATTENUATION WHEN ω_N VARIES WITH TIME

In the attenuation case, an approximate expression for the change in α with N that is good to within 10 percent when $\omega_N/\omega < 0.7$ and $\nu/\omega < 0.7$, is:

$$d\alpha = \frac{81}{4cr^2} \frac{\nu(2 + (\omega_N/\omega)^2)}{1 + (\nu/\omega)^2} \frac{dN}{[1 - (\omega_N/\omega)^2]^2 (\nu/\omega)^2} \text{ nepers/m} \quad (29)$$

For heights between 65 and 150 km and for frequencies above 15 Mc, $\omega_N/\omega < 0.3$ and $\nu/\omega < 0.3$. An appropriate approximation of Eq. (29) in this height range is

$$d\alpha = \frac{81}{2 cr^2} \nu dN \text{ nepers/m} \quad (30)$$

The change in power absorption of a signal in decibels is

$$dA = d [20 \log_{10} \exp (\alpha \Delta S)] \quad (31)$$

For small changes in path geometry

$$dA = 8.66 \Delta S d\alpha \text{ db} \quad (32)$$

Substituting Eq. (16) into Eq. (18)

$$dA = \frac{8.66 (\Delta S) (81) (\nu)}{2 cr^2} dN \text{ db} \quad (33)$$

The change in phase with a change in N for $\omega_N/\omega < 0.3$ is from Eq. (12)

$$d\ell = \frac{d\phi}{2\pi} = \frac{81 \Delta S}{2 cr^2} dN \frac{\omega}{\omega \pm \omega_N |\cos \theta|} \text{ cycles} \quad (34)$$

Now, reasonable values for the PR-SU path geometry are $h' = 300$ km and $d = 5400$ km. Let us assume arbitrarily that $a = 20$ km. The above values, when substituted in Eq. (9), give $\Delta S = 360$ km since, for low takeoff values, $\tan \psi_n \approx \psi_n$.

Let us calculate the effect of a change in the ionization of the D region on the absorption of a 15-Mc signal. At these heights (see Fig. 21) $\nu = 10^7/\text{sec}$; thus, from Eq. (18) one gets:

$$dA = \frac{(8.66) (81) (10^7) (3.6 \times 10^5)}{(2) (3 \times 10^8) (15 \times 10^6)^2} dN = 1.85 \times 10^{-8} dN \quad \text{db} \quad (35)$$

From Eq. (35) the phase change of this signal is:

$$d\phi = \frac{(2\pi) (81) (3.6 \times 10^5)}{(2) (3 \times 10^8) (15 \times 10^6)} dN = 2\pi(3.2) \times 10^{-9} dN \quad \text{radians} \quad (36)$$

The phase change in number of cycles is:

$$\frac{d\phi}{2\pi} = 3.2 \times 10^{-9} dN \quad \text{cycles} \quad (37)$$

In the D region, N is approximately 5×10^9 electrons/ m^3 . A change of 50 percent in N (not unusual during fadeouts) corresponds to a drop in signal level of (from Eq. 35):

$$dA = 1.85 \times 10^{-8} (2.5 \times 10^9) = 4.5 \quad \text{db} \quad (38)$$

and a phase change of (from Eq. 37):

$$d\ell = 3.2 \times 10^{-9} \times 2.5 \times 10^9 = 8 \quad \text{cycles} \quad (39)$$

The absorption would certainly be detectable, but the phase change is barely detectable as a frequency deviation if it occurs over a period of greater than half a minute. The large value of the absorption implies that frequency deviations are due to ionization changes in higher regions.

If the layer is placed at E-region heights (100 to 120 km), $\nu = 10^5/\text{sec}$; then

$$dA = 1.8 \times 10^{-10} dN \quad \text{db} \quad (40)$$

and
$$d\ell = 3.2 \times 10^{-9} dN \quad \text{cycles} \quad (41)$$

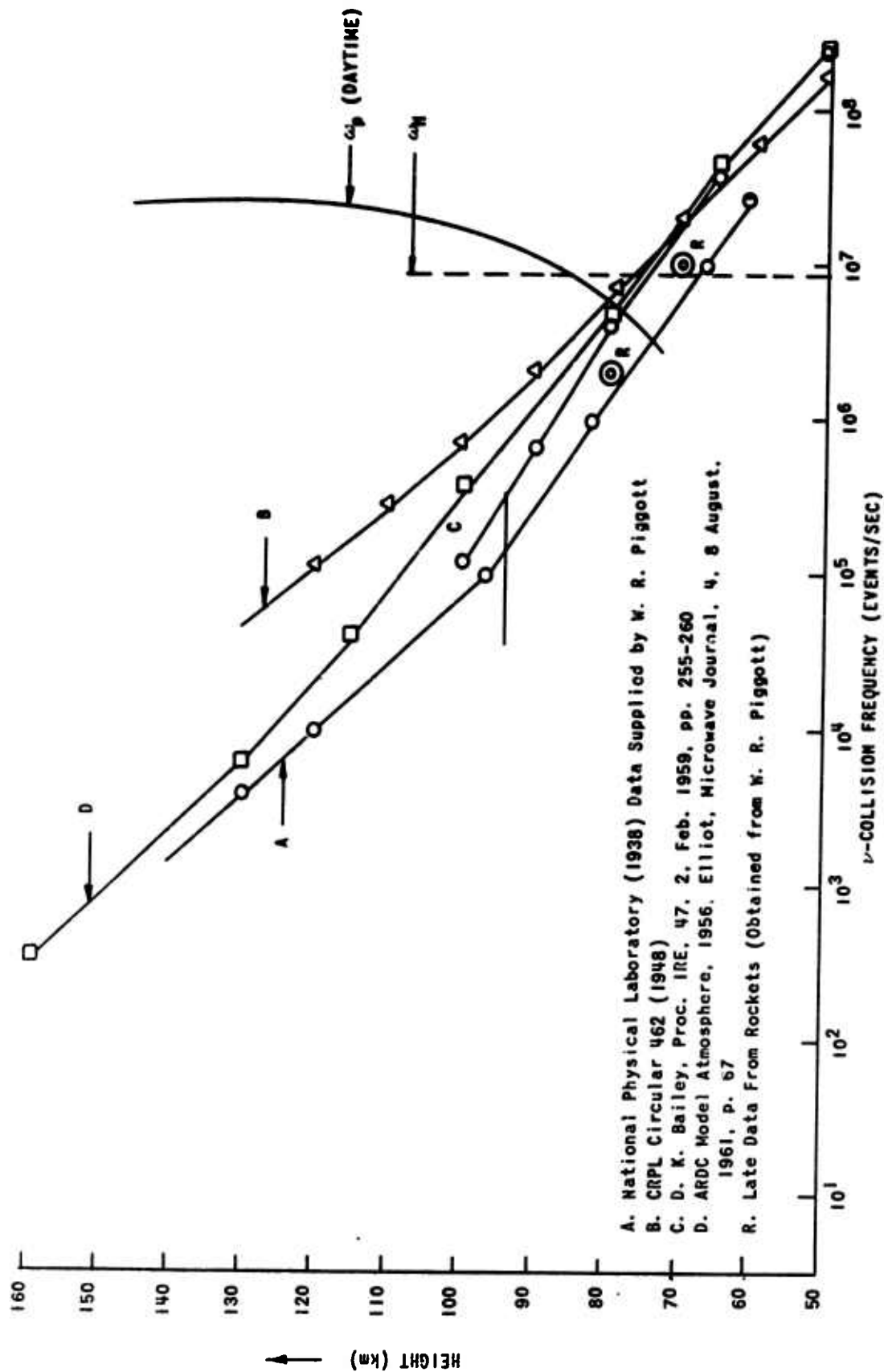


FIG. 21. COLLISION FREQUENCY VS HEIGHT.

For this case a phase change of 120 cycles (or a 2-cps "kick" for 1 min--not unusual, see Figs 3 and 5) would cause an absorption change of about 7 db, an amount easily noticeable. This corresponds to a change of $120/3.2 \times 10^{-9} = 3.8 \times 10^{10}$ electrons/m³, or 30 percent of the E-region electron density.

Since certain solar flares produce phase changes of the above magnitude without any observable absorption, the ionization in these cases must be introduced at a yet higher level. Assuming that changes in signal strength of less than 1 db cannot be distinguished in the present setup, we will calculate the minimum height of the band whose ionization change will produce the observed frequency kicks.

For example, the 14 August 1961 (Fig. 5a) solar subflare produced a phase change of 300π radians (150 cycles) but no observable absorption on the PR-SU 15-Mc signal.

Calculating the maximum ν which will give an absorption less than 1 db, we substitute Eq. (33) into Eq. (34) and obtain:

$$\nu \leq \frac{2\pi f dA}{8.66 d\phi} = \frac{15 \times 10^6 \times 1}{8.66 \times 150} = 1.15 \times 10^4/\text{sec} \quad (42)$$

A height greater than 125 km is required to give a ν of sufficiently low magnitude. Thus, it appears that some solar flares produce ionization above 125 km. It is noted that an ionospheric disturbance of any origin which causes a phase change of greater than 150 cycles with no observable absorption on the PR-SU 15-Mc signal must occur above 120 km.

G ANALYSIS OF THE INDUCED-EFFECTS OF THE 28 SEPTEMBER 1961 SOLAR FLARE OF IMPORTANCE 3

Now let us examine the effects of the solar flare of importance 3 of 28 September 1961 (Fig. 13). Table 2 contains a detailed record of the events that took place during the lifetime of this flare. The information included in the second, sixth, seventh and eighth columns is taken from the High Altitude Observatory's "Preliminary Reports of Solar Activity" [Ref. 26]. The information contained in the other columns is derived from the record shown in Fig. 13.

TABLE 2. OCCURRENCE OF EVENTS OF FLARE OF 28 SEPTEMBER 1961

(1)	(2)	(3)	(4)	(5)		(6)	(7)	(8)	
Time (GMT)	Optical Occurrence	Frequency Deviation	Absorption Average Slow SWF	Fading Rate (cps)		SPA	SCNA *	SEA	
				18 Mc	15 Mc				
2200	Optical onset	Onset at 15 mc Onset at 18 mc	Onset**			Onset	Onset	Onset	
2207 10									
2208 50				0.36	0.50				
2212				0.35	0.45				
2214				0.50	1.60				
2215				0.90	1.30				
2216 40		Maximum 15 and 18		1.70	1.90				
2216 55				1.50	1.40				
2217				1.00	1.00				
2218 12				0.90	0.90				
2218 50	Max Optical Phase	Zero Frequency Max Neg Freq	Max	0.90	1.20				
2221 10				0.40	0.60				
2224									
2226	End			0.20	0.30		Recovery		
2250									
2330									

Importance

3

1

2

1/20X

1

^{*} SCNA = Sudden Cosmic Noise Absorption^{**} The time given by Ref 26 was 2218 GMT

A cursory glance at Table 2 shows the following:

1. The maximum of the amplitude fading rate occurs at the same time as the maximum frequency (phase) change.
2. The absorption starts after the maximum frequency deviation and reaches its maximum some $5\frac{1}{2}$ min later. Even this maximum absorption is classified as one of importance 1, i.e., very moderate.
3. The SPA, SCNA and SEA effects have their onset times 5, 7 and 8 min, respectively, after the onset time of the frequency change, and their importance is of secondary value. It seems that during this flare, ionization was produced at all levels simultaneously (as is the case during very strong solar flares); but maximum ionization was produced first at higher levels (see frequency and absorption maxima about 4 min apart) and then at the lower levels. Even the lower ionization production was not too pronounced, as one can see from the severity of the SPA, SCNA, SEA, and particularly the slow SWF effects.
4. The 15- and 18-Mc signals suffered a total of 1100 and 910 cycles of additional phase rotation, respectively, before any observable absorption was noticed. These values are proportional to $1/f$.
5. The maximum frequency change occurs simultaneously on both frequencies to within ± 0.5 sec. An additional fact that must be brought out here is that the sun is low over much of the path (5 PM local time in Florida, one-third of the way from PR to SU). Also, because

of the proximity of the equinox, the subsolar point is many degrees south of the path. Its rays fall at somewhat grazing angle on the ionosphere through which the PR-SU path passes.

Combining Eqs. (33) and (34), one gets

$$\frac{d\ell}{d\lambda} = \frac{f}{8.66 \nu}$$

For the solar flare of 28 September 1961, the phase change before any observable absorption occurred was 910 cycles at 18 Mc and 1100 cycles at 15 Mc.

The total change in ionization along the path is, from Eq. (34),

$$\Delta S \, dN = \frac{910 \times 18 \times 10^6 \times 2 \times 3 \times 10^5}{81} = 1.2 \times 10^{14} / \text{m}^2 \quad (43)$$

assuming the minimum change in signal level that can be detected is 1 db.

The maximum average value of ν that can cause ≤ 1 db absorption is derived from Eq. (42):

$$\nu = 2 \times 10^4 / 8.66 = 2.3 \times 10^3 / \text{sec} \quad (44)$$

The height with this ν is 140 km; thus, the average height of ionization change is 140 km or more. For a path length of 400 km through the layer (thickness of layer of 20 km), the change in ion density is obtained from Eq. (26) as

$$dN = \frac{1.2 \times 10^{14}}{400 \times 10^3} = 3 \times 10^8 \quad \text{electrons/m}^3 \quad (45)$$

The values given by Eq. (32) are less than 1 percent of the ion density of the region at 140 km. This small value is obtained from the assumption that the layer was 20-km thick. Actually, however, it could be much less than this, say about 2-km thick.

The above analysis could also be carried out by considering the recombination coefficients of the different charged particles for the different heights [Ref. 29]. However, this was not accomplished for two reasons: (1) there are many such coefficients in the lower ionosphere,

and their exact variation with height is not well known, and (2), because of the recording speeds employed during these experiments, the exact recovery times of the frequency fluctuations during solar flares could not be determined with accuracy. As an alternative method, the effect of absorption was chosen since the variation of the collision frequency with height is better known.

II AGREEMENT OF THEORETICAL AND EXPERIMENTAL RESULTS

The previous analysis and experimental evidence indicate that the proposed model of Fig. 20 is a reasonable one, to a first approximation.

Since Ellison [Ref. 30] suggested that during solar flares, intense radiations around 500 and 1200 Å may be emitted (although he states that we have no proof of this) and Friedman [Ref. 31] described rocket experiments which yielded the information that radiations between 100 and 1000 Å are absorbed in the region between 120 to 140 km, one might speculate that during solar flares radiations of this type ionize the upper atmosphere at these heights. The time variation of the ionization change produces these frequency kicks without producing absorption (i.e., without penetrating down to the D or E region).

In the case of vertical-incidence ionograms to determine height of reflection, one must take into account the additional retardation introduced by the extra ionization that is introduced by the solar flare. If this retardation occurs somewhere below the reflection point of the vertical wave, the virtual height will seem to rise; whereas actually this is not so. This can be shown from differentiating the argument of Eq (5) with respect to ω since the time delay is

$$\tau = \frac{d\phi}{d\omega} = 2 \frac{d}{d\omega} \left(\omega t + \int_T^R \beta ds \right) \quad (46)$$

Since ϕ increases during the time interval of a solar flare, τ will be larger and the virtual height will seem higher. Thus, one may draw the erroneous conclusion that the layer rises because of a reduction of the electron density near the reflection point [Ref. 3]. A reduction in the ionization density does not take place during solar flares, since it has been shown that the total ionization of the atmosphere increases by

more than 100 percent during some strong solar flares [Refs. 15 and 22]. This indicates that not only the D-region ionization is increased (as evidenced by the absorption results) [Refs. 2-7, and 14, 19 and 29] or the E region (as shown by Burkard [Ref. 11], Bibl [Ref. 17], and Findlay [Ref. 18]), but the higher levels as well, as shown by the isolated case of Naismith and Beynon [Ref. 12]. Furthermore, from the observation of the frequency of backscattered signals during solar flares, it is concluded that the downward-moving-layer model [Refs. 15 and 22] is not always an appropriate one [Ref. 32].

The following model might then be proposed: During some solar flares ionization of certain band frequencies (UV) arrives first and ionizes primarily the 120- to 140-km height with small increases in the ionization in the D and F regions. Subsequently, the ionization "hardens" (probably because of the arrival of X-rays and gamma-rays) and produces electron-density variations in the D region, which results in absorption.

V. CONCLUSIONS

During the lifetime of certain of the solar flares reported [Refs 25 and 26], the frequency of an obliquely propagated h-f wave in the frequency range between 10 and 20 Mc is momentarily changed by a few cycles. The change consists of an increase in the instantaneous-received frequency, followed by a decrease and subsequently a gradual return toward the original-received frequency. The rapid part of the frequency variations lasts only a few minutes (usually less than 5). In addition, the frequency change varies inversely with the operating frequency, as contrasted with the so-called doppler frequency changes, produced by moving inhomogeneities and traveling ionospheric disturbances, which vary directly proportionally with the operating frequency.

Paths separated by many hundreds of kilometers are simultaneously affected. These frequency changes invariably occur prior to the commencement of the signal absorption (1 to 5 min; on the average of every 2 min). Various degrees of change ranging from no observable absorption to complete signal loss have been observed. The azimuthal angle of arrival of the same signals that suffer frequency changes during some of the solar flares and subflares is also shifted off its true bearing. These bearing deviations are toward the south in the case of the Puerto Rico - Stanford path. They indicate that electron-density gradients are formed when the sun illuminates part of the path or the sun's radiation is falling at a grazing incidence.

These observations of instantaneous-frequency and angle-of-arrival changes during solar flares, together with other experimental results such as backscattered h-f signals, measurements of F-region electron density, and ultraviolet absorption by the ionosphere, suggest that new ionization is introduced initially somewhere just above the E region (very probably in the height region 120 to 140 km), although even greater heights are possible. This ionization may or may not be followed by the generation of ionization in the absorbing D region.

The time variation of the height at which solar-flare-induced ionization is released, suggests that the ionization producing radiant energy is initially soft (500 to 1000 \AA), and then hardens (1 to 100 \AA) as the flare progresses.

The fact that the frequency or phase change comes invariably prior to the signal loss shows that it could conceivably be used to warn of impending signal loss in modern h-f communication systems, affording continuous feedback of propagation conditions over the path.

The short-lived frequency variations caused by ionization changes due to solar-induced radiation, however, should be distinguished from a similar kind that is observed during sudden commencements or sudden fluctuations of the geomagnetic field. These short-lived variations vary proportionally with the operating frequency and affect the different modes (i.e., ordinary and extraordinary) by different amounts. Thus, frequency splitting is observed during these fluctuations which is not observed during the solar-flare-induced, ionization-change frequency shifts.

ACKNOWLEDGMENTS

The authors are indebted to Professor Braulio Dueño and his staff of the University of Puerto Rico, Mayaguez, Puerto Rico; to Professor H. M. Swarm and his staff of the University of Washington, Seattle, Washington; to Professor W. B. Wrigley and his staff of the Georgia Institute of Technology, Atlanta, Georgia; and to the staff of the Radioscience Laboratory of Stanford University, Stanford, California. In particular, they would like to thank Joseph H. Hawkins for building and maintaining the equipment in good working order, and Paul R. Widess for helpful discussions and calculations.

REFERENCES

1. Mögel, H., Telefunken-Zeitang, II, 4, 1930.
2. Dellinger, F. H., Science, 82, 1935, pp 351, 458.
Phys. Rev., 48, 8, October 1935, p. 705.
Phys. Rev., 50, 12, December 1936, p. 1189.
3. Martyn, D. F., et al, "Ionospheric Disturbances, Fade-Outs, and Bright Solar Eruptions", Nature, 140, 9 October 1937, pp. 603-604.
4. Dellinger, J. H., "Sudden Ionosphere Disturbances", Jour. Geophys. Res., 42, 1, March 1937, pp. 49-53; see also Proc. IRE, 25, 10, October 1937, pp 1293-1290.
5. McNish, A. G., "Terrestrial Magnetic and Ionospheric Effects Associated with Bright Chromospheric Eruptions", Terr. Mag., 42, 2, June 1937, pp 104-122.
6. Berkner, L. V., and Wells, H. W., "Further Studies of Radio Fade-Outs", Jour. Geophys. Res., 4, 3, September 1937, pp. 301-309.
7. Bureau, R., "Abnormalities of the Ionosphere and Bright Solar Eruptions", Nature, 139, January 1937, pp. 110-111.
8. Berkner, L. V. and Wells, H. W., "Study of Radio Fade-Outs", Jour. Geophys. Res., 42, 2, June 1937, pp. 183-194.
9. Berkner, L. V., "Concerning the Nature of Radio Fade-Out", Phys. Rev. 55, March 1939, pp. 536-544.
10. Martyn, D. F., "Concerning the Nature of Radio Fade-Out", Phys. Rev. 55, 10, May 1939, p. 983.
11. Burkard, O., "Limiting Waves and the Ionosphere II", Hochfrequenztechn und Electroakustic, 52, 1, July 1938, pp. 23-26.
12. Naismith, R. and Beynon, W. J. G., "Bright Solar Eruptions and the Ionosphere", Nature, 142, October 1938, pp. 250-251.
13. Beckman, B., Menzel, W., and Vilbig, F., "The Times and Appearance of the Dellinger Effect, and its Intensity Distribution on Different Lines of Wireless Communication", TFT, 27, 12, December 1938, pp. 555-560.
14. Bracewell, R. N. and Starker, T. W., "The Study of Solar Flares by Means of Very Long Radio Waves", Mo. Not. of the Roy. Astron. Soc., 109, 1, 1949.

15. Becker, W. and Dieminger, W., "Der Wirksame, Mittägliche Rekombinations-Koeffizient Der FZ-Schicht, Berechnet aus Deren Grenzfrequenzverlauf Während Des Mögel-Dellinger-Effektes A M 19 November 1949", Zs. für Naturforschung, 50, 16, 1950, pp. 308-311, and J.A.T.P., 1, p. 42.
16. Minnis, C. M. and Bazzard, G. H., "Solar-Flare Effect in the F₂ Layer of the Ionosphere", Nature, 181, 4610, 8 March 1958, pp. 690-691.
17. Bibl, K., "'L' Ionization De La Couche-E, Sa Mesure Et Sa Relation Avec Les Eruptions Solaires", Ann. de Geoph., 7, 4, 1951, pp. 208-214.
18. Findlay, J. W., "An Investigation of Sudden Radio Fade-Outs on a Frequency Near 2 Mc", Jour. Atmosph. Terr. Phys., 1, 1951, pp. 367-375.
19. Ellison, M. A., "The H- α Radiation from Solar Flares in Relation to Atmospherics on Frequencies near 27 kc/s", Jour. Atmosph. Terr. Phys. 4, 1953, pp. 226-237.
20. Fenwick, R. C. and Villard, Jr., O. G., "Continuous Recordings of the Frequency Variation of WWV-20 Signal after Propagation over a 4000 km path", Jour. Geophys. Res., 65, 10, October 1960, pp. 3249-3260.
21. Chan, K. L., Villard, Jr., O. G., and Dueño, B., "Observation of Correlated Frequency Fluctuations of WWV-20 and FR-17 as Received at Stanford University, Palo Alto, California and University of Washington, Seattle, Washington", TR No. 23, Radioscience Laboratory, Stanford, California, Contract Nonr 225(33) NR 087 090, 10 January 1961. Also presented in the Fall, 1960 URSI-IRE Meeting at Boulder, Colorado, December 1960.
22. Knecht, R. W. and Davies, K., "Solar Flare Effects in the F-region of the Ionosphere", Nature, 190, 4778, 27 May 1961, pp. 797-798.
23. Watts, J. M. and Davis, K., "Rapid Frequency Analysis of Fading Radio Signals", Journ. Geophys. Res., 65, 8, August 1960, pp. 2295-2301.
24. Kanellakos, D. P. and Villard, Jr., O. G., "Some Relationships Between Frequency and Azimuth Angle of Arrival of H-F Waves Propagated Over Long Distances", Fall URSI-IRE Meeting, Austin, Texas, October 1961, TR No. 43, Radioscience Laboratory, Stanford, California, Contract Nonr 225(33) NR 088 003, In Press.
25. "Solar Geophysical Data", National Bureau of Standards, CRPL-F Series, part B, Monthly Summaries. This publication includes data from many observatories around the world.

26. Solar Flares and Subflares are reported by High Altitude Observatory, Boulder, Colorado, "Preliminary Report of Solar Activity", Weekly Summaries.
27. Ratcliffe, J. A., "The Magneto-Ionix Theory and its Applications to the Ionosphere", Cambridge University Press, 1959, p. 19.
28. Keslo, J. M., "Doppler Shifts and Faraday Rotation of Radio Signals in a Time-Varying Inhomogeneous Ionosphere, Part I. Single Signal Case", Jour. Geophys. Res., 65, 12, December 1960, pp. 3909-3914.
29. Mitra, A. P. and Jones, R. E., "Recombination in the Lower Ionosphere", Jour. Geophys. Res., 59, 3, September 1954, pp. 391-406.
30. Ellison, A. M., "The Sun and its Influence", The McMillan Co., 1955, p. 112.
31. Friedman, H., "Sources of X-ray Emission in the Solar Atmosphere", URSI-IRE Meeting, Washington, D.C., May 1-4, 1961.
32. Widess, P. R. and Barry, G. H., "Use of a Phase-Sensitive Backscatter Sounder to Deduce Ionospheric Changes Associated with a Solar Flare", TR No. 37, Radioscience Laboratory, Stanford, California, Contract Nonr 225(33) NR 088 003, In Press. Abstract presented at Fall URSI-IRE Meeting, Austin, Texas, October 1961.

TEPEE DISTRIBUTION LIST
November 1961

Headquarters, Foreign Technology Div., Wright- Patterson
AFB, Ohio

Attn: ID-A3a

Attn: ID-E1B

Attn: TD-X1A

1
1
1

Headquarters, AF Cambridge Research Labs., Office of
Aerospace Research, USAF, L.G. Hanscom Field, Bedford,
Mass.

Attn: ERD-CRRK Dr. Philip Newman

Attn: ERD-CRRI Mr. Wm. F. Ring

Attn: Dr. G.J. Gassman

1
1

Hq., USAF, Office of Assistant Chf. of Staff,
Intelligence Systems Branch (AFCIN-P2), Washington 25, D.C.

1

Headquarters, USAir Force, (AFTAC/TD-5), Washington 25, D.C.

1

Headquarters, North American Air Defense Command, Ent
Air Force Base, Colorado Springs, Colorado

Attn: NEEC

1

Headquarters, Space Systems Division, Air Force Systems
Command, USAF, Air Force Unit Post Office, Los Angeles 45,
California

Attn: SSZC

1

Headquarters, Rome Air Development Center, AF Systems
Command, USAF, Griffiss Air Force Base, New York

Attn: RALTT-Mr. F.C. Bradley

Attn: RAUEL-3-Mr. B. Cooper

1
1

Headquarters, Strategic Air Command, Offutt Air Force
Base, Nebraska

1

Commanding Officer, U.S. Army Signal Radio Propagation
Agency, Ft. Monmouth, New Jersey,

Attn: SIGRP-B

1

Commanding Officer, U.S. Army Signal Missile Support
Agency, White Sands Missile Range, New Mexico

Attn: SIGWS-PO

1

Office of the Chief of Ordnance, Dept. of the Army,
Washington 25, D.C.

Attn: ORDTU-Dr. C.M. Hudson

1

TEPEE DISTRIBUTION LIST

Commanding Officer, Scientific Liaison & Advisory Group, Rm. 1B657, The Pentagon, Washington 25, D.C., Attn: Mr. Richard A. Krueger	2
Chief, U.S. Army Security Agency, Arlington Hall Station Arlington 12, Virginia Attn: LADEV-S	1
Commanding Officer, U.S. Army Signal Electronic Research Unit, P.O. Box 205, Mt. View, Calif.	1
Commanding Officer, Picatinny Arsenal, Dover, New Jersey Attn: Technical Information Library	1
Diamond Ordnance Fuze Laboratories, Ordnance Corps, Washington 25, D.C. Attn: Walter J. Brinks (Mathematician CCM & Special Systems Branch)	1
Commanding Officer, Army Rocket & Guided Missile Agency, U.S. Army Ordnance Missile Command, Redstone Arsenal, Alabama Attn: Dr. Nils L. Muench	1
Commanding General, U.S. Army Signal Research & Development Laboratory, Ft. Monmouth, New Jersey Attn: Mr. Murray Miller	1
Chief of Naval Operations, Dept. of the Navy, Washington 25, D.C. Attn: Op-70	1
Op-92	1
Op-92B3	1
Op-71	1
Op-733	1
Op-07TE	1
Chief, Bureau of Ships, Dept. of the Navy, Washington 25, D.C. Attn: Code 362A	1
Director, Special Projects, Dept. of the Navy, Washington 25, D.C. Attn: SP-2041	1
Commanding Officer, U.S. Naval Ordnance Test Unit, Patrick Air Force Base, Florida Attn: N3	1

TEPEE DISTRIBUTION LIST

Commander, U.S. Naval Missile Center, Pt. Mugu, California Attn: Technical Library, Code N0302.1	1
Commander, Naval Air Test Center, Patuxent River, Md. Attn: Weapons Systems Test Division (Code 424)	1
*Director, U.S. Naval Research Laboratory, Washington 25, D.C. Attn: Code 5320 Attn: Code 2027	1 1
Commanding Officer & Director, U.S. Navy Electronics Laboratory, San Diego 52, California Attn: Library	1
Chief of Naval Research, Dept. of the Navy, Washington 25, D.C. Attn: Code 427 Attn: Code 463 Attn: Code 420C Attn: Code 418	1 1 1 5
Commanding Officer, U.S. Naval Ordnance Laboratory, Corona, California Attn: Mr. V.E. Hildebrand	1
Chief, Bureau of Naval Weapons, Dept. of the Navy Washington 25, D.C.	1
*Armed Services Technical Information Agency, Arlington Hall Station, Arlington 12, Virginia	10
Director, Weapons Systems Evaluation Group, Rm. 1E875, The Pentagon, Washington 25, D.C.	1
Institution for Defense Analyses, Washington 6, D.C. Attn: RESD-Dr. Paul Von Handel Attn: RESD-Dr. Carlos Angulo	1 1
Director, Advanced Research Projects Agency, Washington 25, D.C. Attn: LCDR D. Chadler Attn: Mr. J. Ruina Attn: Mr. T. Bazemore Attn: Mr. A. Van Every	1 1 1 1

*All requests for this report shall be approved by the
Office of Naval Research (Code 418), Oxford 6-4476.

TEPEE DISTRIBUTION LIST

Director, National Security Agency, Ft. G.G. Meade, Md Attn: CREF-141	1
Director, National Bureau of Standards, Boulder, Colo. Attn: Mr. Richard C. Kirby (Chf, Radio Systems Div)	1
Attn: Mr. L.H. Tveten (HF/VHF Research Section)	1
ACF Electronics Division, ACF Industries, Inc. 3355 52nd Avenue, Hyattsville, Md. Attn: Mr. Wm. T. Whelan (R&D)	1
**Inspector of Naval Material, 401 Water St. Baltimore 2, Maryland	
Aero Geo Astro Corp. 1200 Duke St. Box 1082, Alexandria, Virginia Attn: Mr. D. Reiser	1
**Inspector of Naval Material, 401 Water St. Baltimore 2, Md.	
Radio Corporation of America, Aerospace Communications and Control Division, Burlington, Mass. Attn: Mr. J. Rubinovitz	1
**Inspector of Naval Material, 495 Summer St. Boston 10, Mass	
Stanford Research Institute, Communication & Prop. Laboratory, Menlo Park, California Attn: Mr. R.L. Leadabrand	1
Attn: Mr. D. Neilson (Data Center)	1
Attn: Mr. R. Vincent	1
**Commanding Officer, Office of Naval Research Branch Office, 1000 Geart St., San Francisco, California	
Aero Geo Astro Corporation, 13624 Magnolia Avenue, Corona, California Attn: Mr. A. Waters	1
**Inspector of Naval Material, 401 Water St., Baltimore 2, Maryland	
The University of Michigan, Radiation Laboratory, 201 Catherine St., Ann Arbor, Mich. Attn: Dr. R.J. Leite	1
**Office of Naval Research, Resident Repr. Univ. of Mich., 820 E.Washington St. Ann Arbor, Michigan	

**
 When the document is classified, send a copy of the
 receipt form to this addressee.

TEPEE DISTRIBUTION LIST

Ballistic Missile Radiation Analysis Center, Institute
of Science & Technology, The University of Michigan,
P.O. Box 618, Ann Arbor, Michigan
Attn: R. Jamron

1

**Office of Naval Research, Resident Repr.
Univ. of Mich., 820 E. Washington St.
Ann Arbor, Michigan

Raytheon Company, Communications & Data Processing Ops.
1415 Boston-Providence Turnpike, Norwood, Mass.
Attn: L.C. Edwards

1

**Resident Naval Inspector of Material
Raytheon Manufacturing Co., Waltham, Mass.

Mass. Institute of Technology, Radio Physics Division,
Lincoln Laboratory, P.O. Box 73, Lexington 73, Mass.
Attn: Dr. John V. Harrington

1

Attn: Mr. Melvin L. Stone (Radio Propagation Group)
Attn: Mr. James H. Chisholm (Radio Propagation Group)
**Inspector of Naval Material, 495 Summer St.
Boston 10, Mass.

1

1

Westinghouse Electric Corporation., Air Arm Division,
Engineering Library, P.O. Box 746, Baltimore 3, Md.
Attn: Mr. David Fales

1

**Inspector of Naval Material, 401 Water St.,
Baltimore 2, Md.

Georgia Institute of Technology, 722 Cherry St., N.W.,
Atlanta 13, Georgia
Attn: Mr. Wrigley

1

**Contract Administrator Southeastern Area
Office of Naval Research, 2110 G. St., N.W.
Washington 7, D.C.

Rand Corporation, 1700 Main St., Santa Monica, Calif.
Attn: Dr. Cullen M. Crain

1

**Inspector of Naval Material, 929 S. Broadway,
Los Angeles 15, California

Pickard & Burns, Inc., 240 Highland Ave., Needham Heights
94, Mass.

Attn: Dr. J. Williams

1

**Inspector of Naval Material, 495 Summer St.,
Boston 10, Mass.

University of California, Berkeley 4, Calif.,
Attn: Dr. E. Pinney

**Office of Naval Research Br. Office, 1000 Geary
St., San Francisco 9, California

When document is classified, send a copy of the receipt form
to this addresssee

UNCLASSIFIED

UNCLASSIFIED